

DOI: <https://doi.org/10.24297/ijct.v23i.9549>

Rotitome-G: Principles and design concept of experimental compliant continuum robotic microsurgical endoscopic sarcotome for pixel/voxel-level target access neurosurgery

Gandhi, Harjeet Singh MD, FRCS, FRCSC, MSc (Biomed Eng.)

Orthopaedic surgeon, Ex-Clinical Assistant, Hamilton Health Sciences, Hamilton, Ontario, Canada

Address: Suite 515, 644 Main Street West, Hamilton, Ontario, Canada, L8S 1A1

Cell Phone number (001) 289 244 7261

harjeetg52@yahoo.co.uk

Abstract

The practice of minimal access surgery is widely accepted, and it has become prevalent with improved endoscope design. The traditional microscope in neurosurgery is gradually being challenged by the neuro-endoscope for its direct co-axial vision and direct illumination of the deep-set subcortical pathology. The conceptualized design of ¹Rotitome-G is based on compliant continuum robotic system. The system is a biomimicry of muscular hydrostat anatomy of the elephant trunk, a plant tendril, and many similar structures in the animal world with an infinite degree of freedom. The article describes the functional anatomy of these structures and the extensor expansion of the human finger as applied to the construction and implementation of the Rotitome-G. This flexible microsurgical endoscope integral to its design has unique cutting tool versions and multiple assistive tools passed through single 'target access' burr hole aperture. It is navigable within the surgical space co-relative to the image space to increase precision and improve the volume of tumour resection. The current study is theoretical and further work is in progress to assess its surgical capabilities to bring it to the clinical arena.

Keywords: Neurosurgery, Neuroendoscopy, Optoelectronics, Pixelectomy, Flexible endoscope, Surgical robotics, Micro-Biomimetic systems, Motion path planning.

1.0 Status of neuro-endoscope

There has been a rapid increase in demand for neuro-endoscope as an assistive tool on the instrument trolley of neurosurgeons. The excellence of endoscope in experienced hands results in lower mortality rate, lesser operative time, lesser blood loss and haematoma formation, better Glasgow coma scale, etc. compared to craniotomy (Sayehmiri et al., 2022; Tan et al., 2021). Otherwise, the solo application of a surgical microscope was and is still the best aid to maximize the excision of intracranial tumours. However, the microscopic view is limited to direct co-axial vision and poor illumination due to a divergent light beam from the overhead operating room light source (Du et al., 2022). The deeper the dissection lesser is the illumination of a tumour workpiece to both aided and unaided eyes of a surgeon. The objective end of an endoscope is very close to the workpiece and has a sharp convergent light beam. It improves visibility by illuminating the hard-to-access peripheral space of a tumour cavity, improving surgeon satisfaction and patient-based outcomes (Singh et al., 2018; Tammam et al., 2022; Tuchman et al., 2014). An exoscope provides an excellent view to perform superficial dissection and resect surface brain tumours (Kinoshita et al., 2021). The greatest benefit of a flexible endoscope has been realized particularly in skull base craniotomies to excise tumours spreading across busy anatomy of the cerebellopontine angle (Abolfotoh et al., 2015; Tammam et al., 2022).

Undoubtedly, the better illumination and wider view of hard-to-access sites with an endoscope are resulting in near complete resection of tumour tissue (Singh et al., 2018; Tammam et al., 2022). In the last decade, there have been several studies, including systematic reviews and meta-analyses, which have shown extremely favourable outcomes where a neuro-endoscope has been combined with a microscope (Du et al., 2022; Sayehmiri et al., 2022; Tan et al., 2022). It has helped not only to increase the volume of removed tumour tissue but also reduced operative time, intra-operative complications and post-surgical neurological deficits, and tumour recurrence (Barber et al., 2013; Rigante et al., 2019; Singh et al., 2018; Tammam et al., 2022).

Currently, the rigid neuro-endoscope design comes with 0°, 30°, 70° and 120° view angles at the objective end to increase the field-of-vision of a neurosurgeon. It means multiple endoscopes become part of the laid-out surgical items. Frequently, for a beginner, higher wide-angled views cause disorientation, at its worse 'sea-sickness' like state due to the shifting horizon effect and early surgeon fatigue. Despite the availability of a fixed wide-angle facility, there are always blind spots in the proximal corners beside the entry point that are easily missed. Recently, there had been the introduction of a mechanical switch operated angle shifting rigid rod lens neuro-endoscope, Endo-CAMEleon or EndActive (Karl Storz, Tuttlingen, Germany), specifically for cerebellopontine angle surgery. The uniplanar Endo-CAMEleon objective end is steerable by -10° to 120° is a clever idea but limited by uniplanar

¹ Pronounce as Roti-tome.

vision. The design of EndActive has 160° view, with the ability to select the region of interest for greater focus. Many of the rigid endoscope limitations have been resolved with the introduction of a flexible neuro-endoscope. Its steerable end enhances all-around access and visibility mitigating the issue of proximal blind spots that remains a challenge when operating with a co-axial forward vision operative microscope.

The malignant tumours are hard-to-resect completely because of their rhizoid spread into the adjacent structures. However, even the encapsulated benign brain tumours, such as in the busy anatomy of the cerebellum and-pontine angle, tend to spread through anatomical corridors, insinuating loose normal tissues, frequently adhering to them(Singh et al., 2018; Tammam et al., 2022). Many a time, it can be extremely difficult to reach the periphery of the tumours in such locations with neither a surgical microscope nor a rigid neuro-endoscope for complete resection. Access to a deep-seated subcortical tumour via a transparent tubular retractor transgressing the brain parenchyma in between white matter tracts does overcome the disadvantages of single and multiple-bladed retractors(Y. Zhao & Chen, 2016). The endoport channel-assisted endoscopic approach of short duration is considered safe and helps complete the resection of intraventricular tumours(Moosa et al., 2018; Yan et al., 2021). Nevertheless, constant contact stresses for an extended period upon the adjacent normal tissues increase the likelihood of ischemia. These novel and specialized instruments in practice are without consistent evidence of their efficacy, ergonomic advantages, and safety due to varied reporting and standardization(Aylmore et al., 2022). A flexible neuro-endoscope has certainly improved access to deep-seated lesions in tedious angular spaces. However, the frustrating limitation is when a neurosurgeon is forced to use rigid-straight and rigid-angled instruments to resect tumour extensions. It increases the risk of injury to important neural and vascular structures. There are various multi-hinged endoscope-holding devices available to help the surgeon to perform bimanual tissue resection but an extra hand for retraction of delicate tissue for better access is always appreciated to increase maneuverability to improve resected tumour volume. The application of rigid instruments like the rigid endoscope also limits access to the ceiling of the tumour cavity. The surgeon's anxiety remains whether it contains the residual tumour tissue or the remnant of the capsule undermined by the healthy brain tissue.

At present several types of available individual mechanical instruments; laser and ultrasound-operated instruments for cutting; variable speed side cutting reciprocating aspirators with scissoring action; monopolar and bipolar cautery systems for haemostasis; abrasion of tumour tissues, retraction, flexible suction, etc. are either straight or angled at their working ends(Aylmore et al., 2022; Ebel et al., 2022; Shaikh & Deopujari, 2020). The greatest difficulty is to manoeuvre them safely and triangulate within an unstructured and constrained space(Marcus et al., 2016). In the absence of real-time MRI, doppler ultrasound imaging can complement endoscopic surgery by providing a real-time direct axial image of immediately surrounding brain tissues for the safe negotiation of instruments for tissue resection. Several types of infrared and electromagnetic wireless navigation systems are fast replacing the stereotactic frames for precise targeting of a lesion for solo neuro-endoscopy. There is increasing interest to establish an intimate working relationship of neuro-endoscope with robotics. It is expected to improve surgical dexterity and opportunity for developing machine learning algorithms.

The rigidity of the surgical instruments limits the working flexibility and maneuverability, adding to surgeon fatigue. Whereas the need for an extra pair of hands defeats the original advantage of a steerable neuro-endoscope when applied through a craniotomy larger than a few burr holes. It becomes even more tedious when the position of the scope holder must be adjusted, and instruments must be retrieved and replaced frequently as the dissection and resection proceed. In addition, to the increase in operating time, the repetitive movements increase the chances of injury to the healthy tissue in narrow access deep dissections. There is a cadaveric-based report on synchronous four- or six-handed dissection technique by two surgeons inserting two endoscopes on holders, through two separate portals to improve the visualization, wider field of vision, wider working space, more assistive tools at once in the field for greater tumor clearance(Alqahtani et al., 2014). Although, unlike a rigid neuro-endoscope, a flexible unit has channels for lavage, suction for introducing biopsy forceps, a cautery probe, and laser instruments reaching out to the operating site, but it increases the outer diameter of an endoscope.

The resection of the brain tumours demands meticulous preoperative planning, the best single portal corridor surgical technique, minimal retraction of the brain tissue, and prevention of harm to eloquent structures. In addition, inclusion of several tools during the procedure for maximum resection of tumor volume is a surgical necessity. There is also need for a neuro-endoscope design for easy adaption of a popular navigation system for locating the region of interest and digital tracking of the leading end of the endoscope as well as the cutting instruments. To meet such requirements, based on Cosserat rod theory to construct a compliant or soft continuum robot-based design(Alqumsan et al., 2019; Bhattu & Kulkarni, 2021; Isbister et al., 2021), the development of a flexible steerable neuro-endoscope like the trunk of an elephant can open up an entirely new field of dynamic endoscopic surgery.

The conceptualized design of the experimental flexible microsurgical endoscope Rotitome-G described here is one such newly conceived device. It is an attempt to bring several assistive instruments integral to its design. The objective of this presentation is to describe the principles of developing a surgical endoscope based on a compliant continuum robotic system and several other elements to construct Rotitome-G. And implementation of the

conceived functions theoretically demonstrating the excision of a brain tumour. The workings of Rotitome-G have been discussed in greater detail elsewhere (H. Gandhi, 2022).

2.0 Target access surgery

The length and curve of the traditional skin incision and osteoplastic craniotomy flap are relatively dependent on the desired anatomical access and size of the index intracranial pathology. It is generally larger than the size of the tumour, cyst, or haematoma discovered on Computed tomography and Magnetic resonance imaging. The concept of minimally invasive access was developed to reduce collateral damage and better cosmetic healing. It was in 1984 that a British surgeon coined the term “minimal invasive surgery” (Wickham, 1987). The concept of minimally invasive surgery in the form of minimal invasive craniotomy for neurosurgical approaches being less traumatic was acquired much later (Pernecky et al., 1994).

The reason the first endoscopic procedures were pioneered in urology to view the internal surface of the bladder was ready natural access through the urethral orifice. The rigid cystoscope was first used as a neuro-endoscope between 1873 to 1877 (Abbott, 2004). Takagi used a 7.3 cystoscope for knee arthroscopy in 1918 (Ainger & Gillquist, n.d.). In 1935 Scarff reported a Neuroendoscopy procedure on the third ventricle using a relatively advanced rigid endoscope in conjunction with a cautery electrode and an irrigation system (K. W. Li et al., 2005; Shim et al., 2017). In orthopaedic surgery, it is a normal practice to make multiple portals to scan and attend to the joint pathology using a rigid endoscope. However, it is rather untenable to make more than one or two portals for minimum access craniotomies to avoid damage to functionally crucial brain tissues. Pernecky described endoscopy anatomy of the brain and advanced the concept of minimum invasive neurosurgery (Reisch et al., 2013).

The term “*target access surgery*” is adapted here to neuroendoscopic surgery, where a single burr-hole size aperture is made under image guidance and assistance of navigation tools to target specific anatomy of the brain (H. Gandhi, 2022). Rotitome-G as an interventional micro-endoscope with several assistive instruments would help accomplish maximum resection of the tumour volume through a single burr-hole. While the robot-assisted target access surgery would overcome surgeon fatigue, inadequacies of hand-eye coordination, and obligatory dextrous surgical skills to perform a traditional craniotomy.

3.0 Biomimetic design principles of Rotitome-G

Although it is impossible to exactly replicate the biology of animals into an engineering device, however, the evolutionary characteristics of animals can be translated to complement certain human limitations for surgical work and time-consuming repetitive activities. Several characteristic design features of the Rotitome-G have been adapted from the anatomy and physiology of the animalcule rotifer, the muscular trunk of the elephant, and the plant tendril. In the rotifer, it is the circumferential arrangement of cilia forming the corona and the oral cavity having chitinous plates to cut and chew food particles that inspired the principal cutting-end design of the Rotitome-G (described later). The features of the tubular elephant trunk as a muscular hydrostat (Kier & Smith, 1983) and highly complex movements of the plant tendril form the flexible insertion part of the endoscope, making Rotitome-G a compliant continuum robotic system. Both the elephant trunk and plant tendril have practically infinite degrees of freedom to probe the environment bringing flexibility and precision to the conceptualized multifunctional microsurgical endoscope.

3.1 Trunk, tendril, and tongue

The term ‘muscular hydrostat’ describes a tubular or a solid structure consisting of densely packed muscles in a three-dimensional arrangement with interspersed fibrous connective tissue (Kier and Smith, 1985) in comparison to incompressible fluid-filled cavities and fibre-reinforced compartments called hydrostatic skeletal system. Muscle tissue has the property of isovolumetric dimension keeping its volume the same during contraction. The shortening in length causes an increase in its diameter within the restrictive circumferential deep fascial compartment. Whether it is a tubular proboscis or a solid tentacle contraction of longitudinal, radial, transverse, oblique, or helical/spiral muscles contraction there is corresponding movement leading to shortening, lengthening, dilatation, or torsion of the structure (Kier, 2012; Kier & Stella, 2007). The reason anatomy and function of the elephant trunk and octopus tentacle are copied for constructing soft and compliant continuum robotic systems is that muscular hydrostats are frequently capable of precise and complex bending movements by selective contraction and relaxation of agonist and antagonistic muscles. The various muscle groups are arrayed in such a manner that longitudinal muscles are located as far as possible from the central axis of the structure to increase bending moment and decrease force to optimize energy expenditure. The helical arrangement of the muscle fibres on contraction produces twisting movement and contributes to the stiffness of the structure. In a double helix, if there is a right-handed spiral the other spiral is left-handed to attain clockwise and anticlockwise motion of the structure. They are also placed in the periphery to increase the twisting force.

An elephant’s trunk attains variable stiffness and optimal position in space by forming multiple pseudo-joints for point-to-point motion (Dagenais et al., 2021). The desired geometry of the path is governed by the kinematics of the trunk through the cumulative effect of bending, elongating, and twisting when reaching out for its target. The

bend typically occurs in two stages (Dagenais et al., 2021), resulting in a sinus curvature. The posture is achieved by first bending inward the most distal segment, followed by propagating the proximal segments to protract the end forward. As the proximal segment lengthens it bends upward (positive curvature) taking advantage of its hyper-redundancy. Such versatility and prolonged stable positioning of the end segment are fundamental to Rotitome-C to attain retroflexion as resection proceeds with the enlargement of the tumour cavity. Retroflexion is like "policeman's tip position", where adduction of arm, internal rotation of the shoulder, with extended elbow, with forearm pronation, flexed wrist and fingers is fixed as seen in Erb's paralysis. A similar pose of the elephant trunk seen normally reaching its rider to 'receive a reward' can be a useful endoscopic manoeuvre within restricted spaces as follow-on propagation complementary to an initial sinus movement.

The complex intrinsic arrangement of muscles in the tongue of animals with several degrees of freedom makes it a solid muscular hydrostat, unlike the tubular proboscis of an elephant. The musculature of the human tongue has longitudinal, transverse, vertical, and horizontal bundles, which allow great mobility (Standring, 2008). The intricate arrangement of the muscles gives it the power of protraction and retraction, flexing upwards and downwards, widening and lengthening, twisting, and rolling it. Apart from these precise movements, the combination of muscle actions permits an infinite degree of freedom (Kier & Smith, 1983). It can hold variable soft and stiff positions making it a versatile and steadfast organ, which is an important mechanical feature of the hydrostats, for inclusion in a compliant continuum robotic technology. Of course, what engineers cannot successfully do is control a versatile engineering device with the same precision as an animal organ under the control of the central and peripheral nervous system.



Figure 1. A segment of a vine showing spiralling tendrils.

The tapered whip-shaped tendrils of the climbing plants are slender solid continuous structures (Fig. 1). In search of steady support, the tip of a tendril oscillates to follow roughly an ellipse drawing partly a spiral and partly a circular path. This revolving climbing motion of a growing tendril or other plant organs is called circumnutation (A. H. Brown, 1993). Circumnutation is a complex energy efficient movement on the fly process of searching the immediate environment by the tendril's sensory-motor end-effector organ (Ceccarini et al., 2021), upon which path planning of a robotic end-effector can be mimicked. The key function of the sensory-motor exploration by the tip of the continuous compliant structure of the tendril is to locate an upright supporting target. In doing so the tendrils tend to oscillate either clockwise or counter-clockwise or the tip may trace a figure-of-eight path. Once engaged successfully, there is a differential growth of the concave and convex sides of the tendril like concentric-flexion and eccentric-extension aspect of a finger to hook around a cylindrical object. This is followed by rapid longitudinal growth of the tendril to generate hyper-redundancy and spiralling to apply forward antigravity traction. The phenomenon of circumnutation is of interest in the construction of the tendril component of Rotitome-C for exploration of space, deciding trajectory and the positioning of its cutting head during preoperative path planning.

The gross anatomy of the proboscis consists of hundreds and thousands of subcutaneous short and long muscles in crucial orientation from its proximal to the distal end. Other than the infinite degree of freedom and excellent grasping skills, the musculocutaneous proboscis of an elephant has suction and spraying abilities. The muscular hydrostatic mechanism helps to perform endless multi-directional movements of protraction, retraction, and curling beyond 180 degrees, varying the compliance along its length (Hannan & Walker, 2003). The grasping

characteristic does not form the function of Rotitome-G, but it is important as far as the effective angular positioning for the cutting end of the endoscope in constrained spaces. The characteristic anatomy and physiology of the elephant's trunk and the plant tendril provide the idea of a semi-soft tubular wall of the Rotitome-G's continuous serpentine body motion. The intramural assembly of several components forms its assistive instruments. There are fibre optics of the camera, space illuminating light emitting diodes; actuating and sensory components, all securely sandwiched within the inner and outer surfaces of the trunk. The tendril carrying the cutting end runs coaxially within the proboscis of the instrument.

3.2 Anatomy and Function of extensor tendon expansion

Although different from the mechanically rigid robotic systems, but central to the fabrication of any compliant or soft continuum robot are its intrinsic support structures. It is generally made up of soft or semi-rigid materials, and hybridization of extensile and non-extensile machine components to control movements in space. The idea of an infinite degree of freedom arises out of the realms of biological structures to manipulate external objects. When it comes to the human interface to the external environment the structure and function of the hands provide an excellent example of biomimicry by modifying the flexion and extension tendon anatomy of a finger as an end-effector organ. In this regard, the anatomy of the extensor tendon apparatus is fully optimized to attain functions in unstructured and constrained spaces. Hence the biomechanical anatomy of the human finger can be easily applied to construct a segmented compliant continuum robot. A segmented cylindrical compliant continuum robot with several degrees of freedom does not have true palmar and dorsal surfaces. Therefore, here the included extensor tendon expansion design performing the agonist and antagonist function is called the extensor-flexor tendon expansion complex. The lateral edge of the expansion on either side receives slips equivalent to lumbrical and interossei muscles effectively causing complex movements like that of a finger.

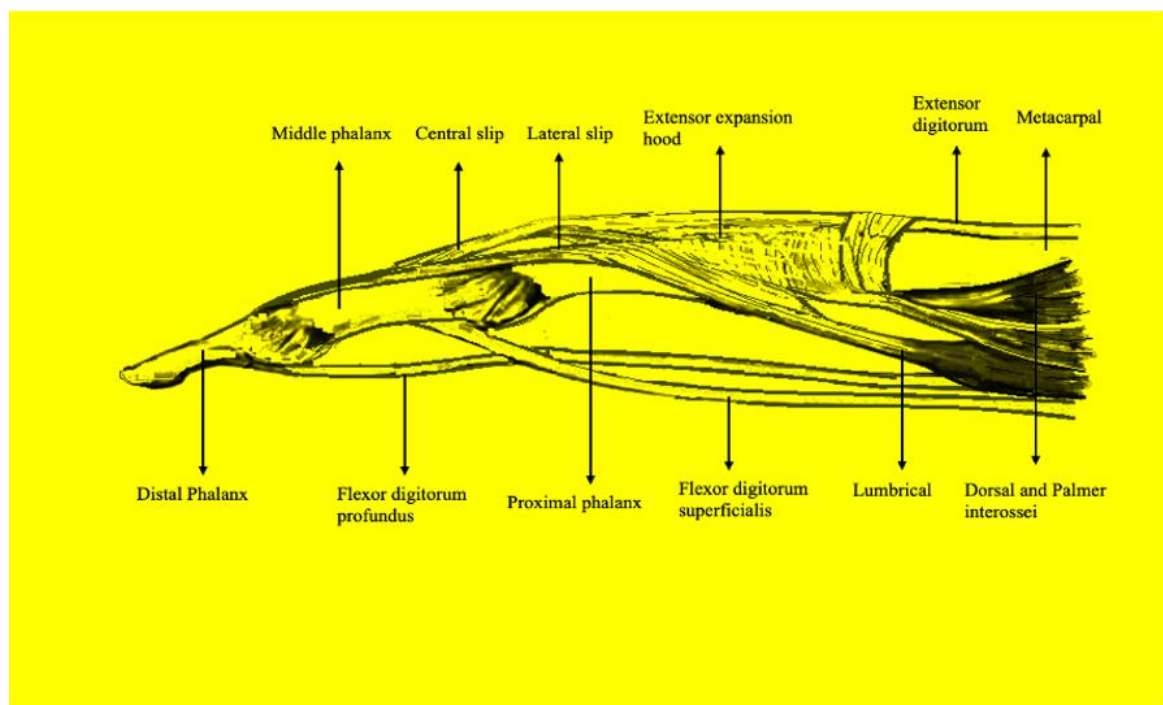


Figure 2. A lateral view of one half of the extensor expansion hood and long flexor tendons of a finger (Modified from Standring, 2008).

The foundational anatomy of each human finger consists of three phalanges [Fig. 2]. The proximal phalanx articulates with the corresponding metacarpal. The coordinated movements of the fingers are made by a complex arrangement of extensor and flexor muscle tendons (Standring, 2008). In the dorsal space of each finger, the extensor tendon apparatus forms an intricate multitailed triangular expansion, with its base at the metacarpophalangeal (MCP) joint holding a central position insert into the middle and distal phalanges. It is held centrally by intrinsic muscles, palmar and dorsal interossei, and lumbricals by their tendons merging on either side of the extensor expansion [Fig. 3]. This arrangement provides complimentary movements at the metacarpophalangeal and interphalangeal joints, variable stiffness, and stability at each joint to hold the finger in a steady attained position. The flat fibrous expansion of the extensor tendon moves distally and proximally over the dorsum of a finger with flexion and extension of the finger respectively. The movement occurs in conjunction with

active movement of the flexor digitorum superficialis and/or flexor digitorum profundus depending upon which of the three phalanges of a finger are engaged in a flexion movement. Unlike a finger with hinge interphalangeal joints

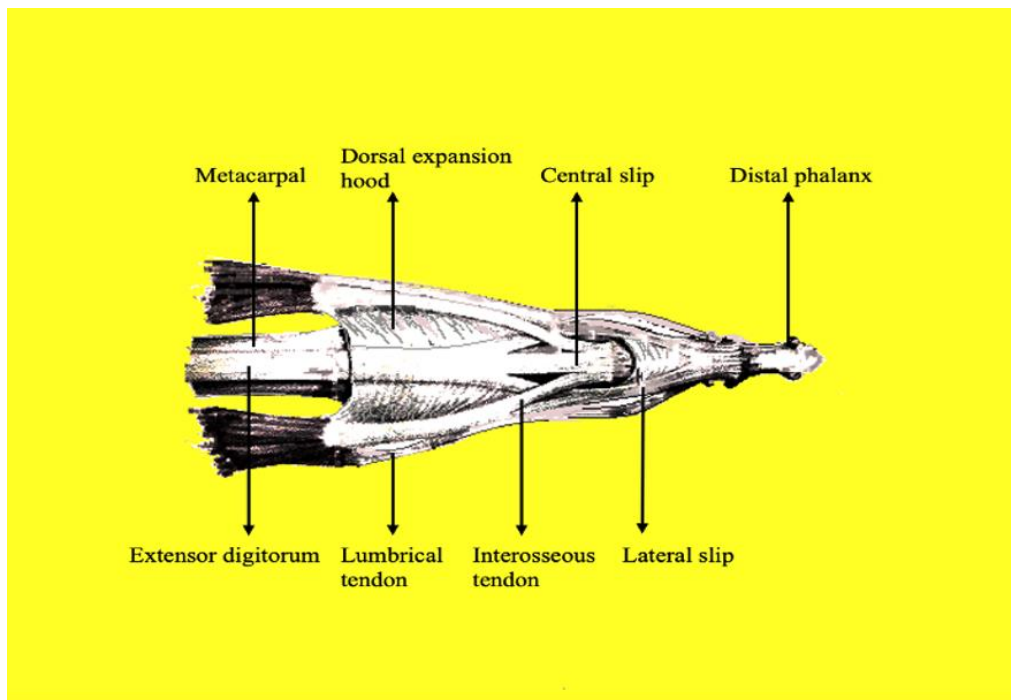


Figure 3. Dorsal view of a finger showing extensor expansion hood, its division, and tendons of lumbricals and interossei muscles merging into its complex anatomy (Modified from Standring, 2008).

for pinching, gripping, grasping, hooking, and poking functions, a compliant continuum robotic system is expected to perform flexion, extension, retroflexion, sweeping, and grazing movements like writing and painting, roughly within a spherical space, given 'infinite' degrees of freedom.

The extensor digitorum muscle in the forearm powers the extensor expansion to the base of the distal phalanx in line with its central axis. The distal end of the extensor digitorum splits into three slips over the proximal phalanx (Stevanovic & Sharpe, 2017). The central slip inserts at the base of the middle phalanx and the lateral slips travel distally, blending to insert into the base of the distal phalanx. The margins of the triangular hood are thickened by the merger of palmar and dorsal interossei on both sides close to the base of the proximal phalanx to join the central slip. The lumbricals merge further distally close to the proximal interphalangeal joints to the lateral slips of the extensor digitorum mechanism (Fig. 3). The interphalangeal (IP) joints are simple hinges, whereas the metacarpophalangeal joints have a greater degree of freedom. The head of a metacarpal bone articulating with the proximal phalanx has a longer diameter in the dorsal to palmar axis than the longitudinal axis. This Cam design increases the joint offset and extent of joint surface helping fingers to reach deeper into the palm to close on an object strongly. The range of flexion and extension at the finger joints is greatly restricted by corresponding opposing muscles (Standring, 2008).

The versatile joint architecture and the arrangement of the ligaments offer variable stiffness and stability to the metacarpophalangeal joint in a closed joint position (full extension) and a variable open position (range of flexion movement). In the open position, the metacarpophalangeal joint has the freedom of flexion, extension, adduction, abduction, circumduction, and limited rotation by complex action of flexors, extensors, lumbrical, and dorsal and palmar interossei muscles (Standring, 2008). The rotation at the MCP joint is because of the combined action of the flexors and extensors when grasping an incompressible object firmly. During flexion and extension of the metacarpophalangeal and proximal and distal interphalangeal joints, the complex distribution of tendons plays a crucial role in coordinating synchronous movements of the phalanges. The lumbricals arise from the flexor tendons and interossei from the metacarpals. The lumbricals insert further distally than the interossei into the lateral tendinous slips of extensor expansions. For stability of the joints simultaneous flexion and extension is essential. The lumbricals and interossei are primary flexors of the MCP joint, at the same time extending the IP joints with rotation at the MCP joint to oppose a finger against the thumb for fine movements, such as writing and drawing. In addition, the lumbricals acting between flexors and extension tendon expansion play a much greater dynamic role in pulling the flexor tendons distally to permit greater extension of the interphalangeal joints. The lumbricals with their longer muscle fibres and tendons are believed to play role in proprioceptive feedback (Standring, 2008). The

network of tendons and ligaments acting on the joints participate in defining finer movements. This complex anatomy and kinematics of fingers can increase the scope of rudimentary flexion and extension movements in a soft and semi-rigid-compliant continuum robotic system. In addition to the flexion and extension movements inclusion of oblique and helical chains of sinews can help attain torsional activity at the end-effector organ of a robot.

The skeletal muscles work by applying tension at their insertion site on a bone close to a joint. The function and force needed to move a joint decide the form and shape of muscles acting on it. The maximum force and function of a limb segment is an anatomical evolutionary optimization process, so to speak, that has followed the principles of the mechanical lever system prevalent in machine design. In designing the compliant continuum robot these structural principles are essential for the best possible mechanical advantage. Virtually all body movements are caused by the coordination of an opposing group of muscles. They contract simultaneously as an agonist and antagonist muscles controlled by motor centres in the central nervous system (Hall, 2016a). It is the relative position and action of these muscles to the central axis that decide the position of a particular segment of an extremity. The force of opposing muscles depends on the load, which decides its position in space, overall stability, and variability in stiffness of the joint under action. During isometric contraction of the voluntary skeletal muscle, there is no shortening in its length, and does not shift the load in space between two points. In comparison, the isotonic muscle contraction causes a shortening against resistance and inertia to move the load in space to the required station. Whereas the isometric muscle contraction is independent of inertia to simply hold the load in its position in space applying force equivalent to the load. Skeletal muscles are composed of numerous muscle fibres. Like fibre, yarn, and the cables to form a rope with its shrink wrap, each of the muscle fibre is successively made up of smaller subunits of myofibrils, which in turn are made up of myosin and actin filaments. Myosin and Actin filaments are arranged in a telescopic fashion as the causative unit responsible for muscle contraction (Heckman & Enoka, 2012). The cell membrane of each myofibril is called sarcolemma. The outer layer of sarcolemma is made up of thin collagen fibrils at each end of the muscle fibres that come together into bundles to form the muscle tendon connecting the muscle belly to its insertion site on the bones.

Where most complicated skills are needed motor and sensory systems are integrated at all levels of activity under the control of the central (brain and spinal cord) nervous system (Hall, 2016b). The sensory system continuously sends feedback from the effector end muscle and tendons serving the mobile bone and joint of a given segment of one or more fingers and the whole extremity depending upon the task (Prochazka & Ellaway, 2012). There are two types of sensory receptors. One that is distributed within the belly of a muscle is called muscle spindles and the other in the substance of its tendon is called Golgi tendon organs. Both send information about the rate of change in length and tension to coordinate flexion and extension of the joints, as well as the position of the affected segment of the extremity in space, often referred to as a proprioceptive function of the sensory system (Proske & Gandevia, 2012). The smooth contraction of a muscle belly is due to the satisfactory response of the muscle spindles. It occurs at the level of the spinal cord in the form of a spinal reflex, otherwise, the contraction would get erratic (Hall, 2016b). The normal process to prevent irregular oscillations is called damping by averaging the feedback signals. It is the function of the muscle spindles to send regular signals to smooth the muscle contraction to stabilize the joint under action and correctly position the limb segment in space. The highly coordinated operation of opposing muscle groups (extensors and flexors; adductors and abductors; pronator and supinator acting as rotators) acting on the joint/s become tense and varies throughout the movement for purposeful positioning of the segment in space to permit variable stiffness. All skeletal muscles are voluntary muscles. The smooth involuntary muscles of soft tubular structures have intramural circular, radial, longitudinal, oblique, and spiral muscle arrangements to cause corresponding movements.

The versatility of human extremities is because of joint design and segmentation of their anatomy into long and short bones. Despite that the hip joint is a universal ball and socket joint, it has only six degrees of freedom and the shoulder has much greater freedom with a greater range of motions in all planes. It is the combined movements of all the segments and variable joint design of the upper extremity that makes it more versatile than the lower extremity. The hand can reach the upper back by adducting, internally rotating the shallow ball and socket of the shoulder, flexing the hinge of the elbow, extending the wrist, and supinating the forearm. The force and coordination of the entire body's muscles can be judged by observing the movements of a baseball pitcher. The concentric contraction of the agonistic muscles effectively elongates the antagonist muscles in a state of eccentric contraction to stabilize the intervening joint/s holding adjacent segments stiff in the desired position. It is an important variable stiffening strategy for attaining stability during motion. In addition, the efficiency of the muscles is increased by enclosing each functional muscle group within individual compartments separated by non-extensible fibrous septae. Finally, the entire limb as a segment of the body is enclosed within non-expansile circumferential deep fascia. It is the interlacing of orthogonally arranged fibres of the deep fascia and the sparsely distributed spiral fibres that provide an anisotropic mechanical advantage. Because of this complex arrangement the non-expansile circumferential deep fascia works like a Chinese finger grip or trap [Fig. 4]. The gripping mechanism comes into play when it is stretched longitudinally. The applied tension reduces the angles between fibres of the fascia/braid decreasing the circumference, pulling it tighter around the muscles or an object. The tension force is converted to compression, making it a predictable and efficient machine. This simple mechanism

can be easily applied to a compliant continuum robotic actuation system for stability and variable stiffness with the shared energy of other parts of the system.



Figure 4. Chinese finger grip. Pulling the chain at its free end tightens the grip over the finger.

Prevention of accidents during endoscopic robotic surgery due to the error of instrument navigation and planning of the trajectory of the end-effector at the pixel or voxel-level resection is a joint engineering and iatrogenic problem. Therefore, the shape and force measured at the sensors and devised trajectory pathway is the result of mathematical algorithms to control important features of robotic surgery (Howie C et al., 2005). The best path planning to develop the patient-specific and patient-appropriate simulation is an interdisciplinary endeavour that must be accomplished at the time of the pre-operative stage.

4.0 Actuators, sensors, and materials for control of a compliant continuum robotic embodiment

Rotitome-G is distinct from the much-described designs of rigid and currently popular interest in soft robots, which are designed for grasping, moving, and positioning small and large industrial items. There is a commonality of functioning elements within the embodiment of all robotic systems, which applies to the functional architecture of Rotitome-G. With the development of newer flexible materials and manufacturing of sub-millimetre and sub-nanometre engineering products, there is a growing interest in the restructuring of rigid robots into hyper-redundant soft and compliant continuum systems with discretely arrayed components (Kato et al., 2016; Ota et al., 2009; B. Zhao et al., 2018). A compliant continuum design has several sub-millimetre-sized components arrayed for a cumulative effect, such that the system conforms to a geometrically accurate angular and linear path to a desired target following a geometrically defined set pathway bit-by-bit with learning capability (Renda et al., 2018).

4.1 Force transmission and actuating materials

There are several kinematic strategies for designing actuators depending on the design, structural configuration, size of the embodiment, and objective functions. It is extremely difficult to replicate the anatomy and physiology of muscular hydrostats with almost infinite degrees of freedom in confined surgical spaces. The iterant multidirectional flexion, extension, retroflexion, protraction and retraction, and torsional movements with variable stiffness are key functions sought in a surgical endoscope. The actuators are transmission units to transmit force to drive the end-effector ergonomically with minimal constraints and energy expenditure. And relatively realign the proximal segments for their optimal positioning.

The actuators and sensors are mechanical and electronic modules, the former as muscles to move the segments of a compliant continuum system and the latter for feedback control of the former. In principle, they should match the flexibility and stretchability of the robot, tolerate millions of cyclical motions, and be fail-safe during its lifetime. All the components should be non-ferrous to be compatible with magnetic resonance imaging in the operating theatre (Kim et al., 2017). There are several varieties of electrical and non-electrical actuators acting as artificial muscles. The actuators have been broadly classified in one of two ways, one based on the mechanically driven soft, elastic, and malleable components, including cables and tendons, fluid-driven chambers, electroactive polymers, shape-memory alloys, springs, and DC servomotors; the second group for force transmission is based on 'muscular hydrostats' and 'hydrostatic skeleton' mechanisms such as tongue, proboscis, tentacles, and tendrils, and even seahorse tail (S. Li & Hao, 2021). The former group includes disks to constrain the tendons and cables like pulleys of flexor tendons in fingers and parts of rotational and universal joints made of soft and elastic materials. The actuators of soft robotic systems are integrated and widely distributed throughout the structure (Trivedi et al., 2008).

There are tendon- or cable-driven actuators (Camarillo et al., 2008; M. Li et al., 2018), such as pneumatic or fluidic actuator McKibben artificial muscle, shape-memory alloys, electro-active polymers (Choi et al., 2005); vacuum jamming of granules by pressure-friction-stiffness of desired segment (Langer et al., 2018). The flexible skeleton of a compliant continuum robot with steel or shape memory Nickel-Titanium (NiTi) springs has inner and outer helical springs (F. Feng et al., 2020). The actuating tendons/cables are confined within the outer spring. The springs as muscles follow Hook's force and displacement principle. They can be an extension or compression type and their torsional rigidity can be controlled by altering their stiffness (F. Feng et al., 2020; M. Li et al., 2018). Tendon actuators are preferred in miniature continuum robots because of installation problems. The materials employed for compliant joint discs are often made of shape-memory NiTi alloy and polyethylene to constrain and direct the cables (Dong et al., 2016; Hao et al., 2017). Acrylonitrile butadiene styrene (ABS) is lightweight and is a preferred material for making rolling joints where the central axis is mobile during bending and torsional movements. However, the friction between the cables and the disc is hard to ignore.

A braid meshwork actuator is constructed with flexible non-extensile material. It has a helical arrangement of fibres with radial and longitudinal cables embedded in it. Its stiffness is controlled by agonist and antagonistic actuators (Hassan et al., 2017). The form of the braid should be cylindrical as suggested above in the form of a Chinese finger grip for the uniform snug fit enclosure to prevent bowstringing or buckling redundancies during flexion losing stabilizing traction force. The stiffness characteristics can be altered by either changing the material properties, the weave of the braid, or traction force on a different combination of tendons. Most of the actuator systems in practice are driven by pneumatic and hydraulic pressure by altering the shape and size of the containers are akin to hydrostatic skeletons. Shape-memory alloys are temperature-dependent and electroactive polymers with embedded electrodes when stimulated respond by extending and contracting (Gu et al., 2017; C. Yang et al., 2020; Youn et al., 2020). Pneumatic artificial muscle by the name of McKibben actuator is made up of an inflatable flexible chamber enclosed in a flexible double-helix braided fibre or elastomer sleeve (Y. Feng et al., 2021; Tondu et al., 1994). They are highly extensible and adaptable low-power actuators. The contraction, elongation, and stiffness direction of its action can be altered by changing the weave geometry and shape of the embracing braid (Klute et al., 1999). The pre-contoured concentric tube actuators (Webster et al., 2009) are made of super-elastic shape-memory metal and polyamide that are coaxially nested together. They can be translated and rotated on a neutral axis to vary the curve and protracted telescopically, having a diameter of 0.8mm for inclusion in sub-centimetre devices (Webster et al., 2006).

Electric-active polymers are low-weight, with high fracture tolerance, having pliable large strain values (Meijer et al., 2001). They come as dielectric elastomers, conductive polymers, carbon nanotubes, etc. The dielectric elastomers are believed to be closest to animal muscles based on criteria of strain, actuation pressure, density, efficiency, and speed (Pelrine et al., 2017). Dielectric actuators made of thin polymer film are coated with compliant electrodes. Although elastomers are nearly incompressible, when an electric field is generated, the sandwiched elastomer reacts by changing in all three planes (Youn et al., 2020). Because of their fast response, they are future candidates for artificial muscle in compliant continuum robots. They are soft, transparent, and lightweight materials having high energy density and can be fabricated into micro-actuators with photolithography (Gu et al., 2017; Yun et al., 2020).

Polymeric filaments and natural fibre and yarn are excellent materials for making flexible actuators (Y. Yang et al., 2020). Woven, knitted, and coiled filaments, fibres, and yarn in a variety of orientations can provide large bidirectional tensile and/or torsional output depending on the configuration of filaments due to contraction and expansion. Polyethylene, nylon, graphene, and carbon nanotubes have been investigated to make wearable devices. Interestingly, the carbon nanotube can be fabricated into continuous material. For designing customized flexible actuators and sensors textile industry standard warp and weft weaving technique is used for weaving the yarn into conducting polymer pieces. The knitted composite spandex and carbon nanotubes have demonstrated tremendous tensile contraction delivering high work density and power output (Foroughi et al., 2016).

Considering the greater tensile strength of silk than steel for a given weight and volume, it is a less explored material for actuator transmission and electrical conduction. It can be woven in a variety of weaves to make meshwork. Recently, resilient silkworm silk and spider silk are finding several applications in electronics as conducting and sensing materials (Steven et al., 2011). The spider silk fibre is stronger than silkworm silk and is more elastic, with a strength higher than that of steel and Kevlar, and more flexible than nylon (Vollrath & Knight, 2001). Stronger than spider silk is Flax with a maximal ultimate tensile strength of 2GPa. The spider silk fibre has a mean diameter of 70 nano microns. The synthetic spider silk can be spun electrically into films and scaffolds for boosting tissue regeneration and repairing ruptured ligaments and tendons (Sionkowska, 2011). The polymeric silk fibre synthesized by insects is a complex protein. The silk fibre of a spider differs from that of the silkworm because of different amino acids in the chains forming the proteins conferring greater toughness, elasticity, and strength to it. Although the native mechanical properties of silk fibre primarily depend on the structure of protein complexes; however, the strength of a ready product for use is the result of the weave and spinning conditions (Vollrath et al., 2001).

The electrically spun mats and individual nano fibres of the synthetic spider silk have found applications as piezoelectric and mechanical sensors. The property of piezoelectricity is due to the vibration of nanosized crystals dispersed in the protein matrix of the silk and is suitable as a mechanical sensor as it undergoes uniform mechanical deformation because of its linear relationship to applied voltage (Karan et al., 2018; Shehata et al., 2018; Steven et al., 2011). The silk fibre can be coated with gold to form a superconducting electrode without eroding the native properties of the silk material. Even though silk is relatively a poor conductor of electricity, it still provides an excellent bed for carbon nanotubes as electrodes (Steven et al., 2013). The spider silk fibre possesses a torsional shape memory that does not require a new stimulus like the shape memory metals to return to its original state (Emile et al., 2007; Kumar & Singh, 2014). Based on mechanical properties, spider silk fibre can be one of the materials of choice for making actuators and sensors in compliant continuum robots (Table 1. See appendix).

The elaborate structure of spider silk structure and its electrical functional capabilities makes it a practical natural high-performance fibre for application in robotic systems.

4.2 Sensors

Active feedback is an essential feature of compliant continuum robotic systems. It is measured as a change in electrical resistance, which varies with applied force to a strain gauge. A strain gauge is an engineering sensor embedded in an object to measure the change in mechanical quantities when external forces are applied to it. It is like receptors made of proteins in biological systems for positive and negative feedback mechanisms that respond to chemical signals. There is a variety of sensors to measure displacement and deformation that occur because of extension, flexion, and torsion providing feedback to control the function of the actuating system. Ideally, a sensor should be submillimetre in thickness, matching the compliance of the robot and high fracture strength. The sensing system can be applied extrinsically on the surface or embedded intrinsically in the substance of the actuators (S. Li & Hao, 2021) respectively can be called exteroceptors and proprioceptors. They come as shape sensors, deflection sensors, force or torque sensors, electromagnetic sensors, and pressure sensors. For widespread response, the sensors can be embedded in thin silicone and polymer film, often called transducers, for estimation of shape and force and applied as double helix strips. Magnetic sensing devices are embedded in a matrix of elastomers for bidirectional control (Luo et al., 2017). Optoelectronic sensing devices depend on the amount of loss of signal as the actuator changes its shape (H. Zhao et al., 2016). The antagonism of an opposing group of actuators is another method for active concentric contraction and active eccentric contraction and active contraction and passive elongation as stimulus-response feedback sensing mechanism (Manti et al., 2016; Ozel et al., 2016).

4.3 Actuating power systems

There are several actuating methods to power soft robotic systems, including shape-memory materials, McKibbin fluidic systems, etc. Electromechanical systems have worked well for a long time in wearable devices with cantilevers, gears, rotary motors, joints, springs, etc. The traditional miniaturized DC servomotors as micro-components are finding application in compliant continuum robots (Barth, 2000; Song et al., 2006). With their rotary function of winding and releasing the force transmitting tendon or a cable actuator can wind around a pulley to apply traction and let go movements causing flexion and extension; protraction and retraction as an active-active or active-passive actuator. The proportional-integral-derivative controller adjusts the length of each active tendon (Gifari et al., 2019).

This highly strategic task is a computational problem to control the actuation and sensor mechanisms to achieve exact positioning, velocity, and force acting on a biological workpiece during surgery by leading the end-effector segment and proximal segments. The same kinematic principles apply to Rotitome-G compliant continuum robotic system without segmental redundancies when acting on a tissue workpiece, without trailing space occupying redundancies inherent in soft robots. The precision activity of Rotitome-G requires uninterrupted work efficiency, without time redundancies during surgery. Therefore, the computational control must be a precise, in-built program to optimize the task for each pathological lesion at the time of pre-surgical planning within an unstructured space. So that the tumour resection proceeds by controlling the movements of the end-effector segment accurately. The path of the iterant movements of the cutting end can only be learned precisely and accurately by defining the precise positioning of the feedback sensors on the actuator system like muscle spindles and Golgi-tendon apparatus for proprioception as mentioned above. Several options of control systems are available for precise modelling of compliant continuum systems for efficient and accurate control (Chikhaoui & Burgner-Kahrs, 2018; George Thuruthel et al., 2018; Marchese et al., 2014) to assist with an instant visual adroitness of an operating surgeon. Further discussion on the computational control methods is beyond the scope of this study.

An accurate positioning and coordinated motion of compliant continuum robots remain a conundrum for control programming and algorithms. Unlike rigid systems, compliant systems do not follow strict three-dimensional cartesian coordinates. Compliant sensors and actuators usually with viscoelastic material properties come with inaccuracies. It is due to non-linear dynamics causing hysteresis during the relaxation phase, which makes it difficult to design easily controllable devices out of such materials. The incorporation of flexible and stretchable silicon-based integrated circuitry in conjunction with micro-mechatronic systems (T. Li et al., 2019) as actuators

and sensors together with carbon nanotube electrodes can bring greater precision into sub-centimetre-sized medical and surgical instruments.

5.0 Structure of the Rotifer

Rotifers are exquisite metazoans, 50–2000 micrometers in length (Trout et al., 2002; Wallace, 2002) [Fig. 5]. The highly concentric arrangement of the cilia around the oral opening of the rotifers gives it a crown-shaped appearance, which is one of the principal design features of Rotitome-G. It is fascinating to watch the cilia beat in tandem, one after the other, giving it the appearance of a rotating wheel, hence, its name rotifer (Wallace, 2002). The incredibly fast beating of the cilia gathers food particles and directs them into the oral cavity. The central oral cavity has chitinous plates that chop and masticates particles before ingestion. This mechanism has been acquired to design one of the cutting tools of Rotitome-G. It is the cutting of soft tissues that makes Rotitome-G a sarcotome (soft tissue cutter).

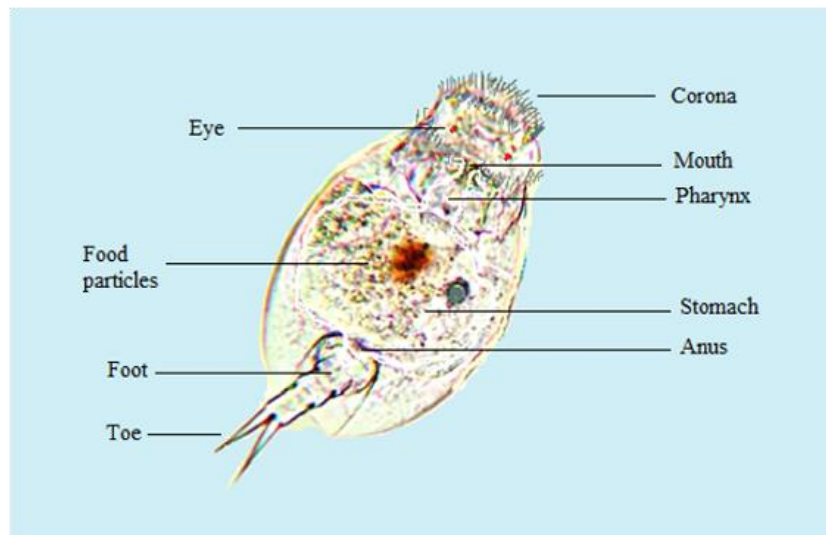


Figure 5. Elementary functional anatomy of a rotifer animalcule as related to the Rotitome-G, showing corona lined with cilia, eyes in red, mouth, stomach, and anus (H. Gandhi, 2022); (The author holds the copyright to republish the image).

The arrangement of sensory organs, eyes, feelers, etc., on the head of the animalcule, are similarly arranged on the end face of Rotitome-G to enhance its working capabilities, making it a multifunctional device.

The working end of the Rotitome-G endoscope is designed with two cutting head variations, one with circumferentially arranged filaments and the other is an iris-shutter cutting mechanism to attain its pixelwise and voxel size piecemeal resection of a tumour.

The ability to introduce Rotitome-G through a single skin portal or a burr hole-size craniotomy aperture to 'target' a lesion under image guidance and computer navigation within closed body cavities in constrained spaces makes it a 'target access' surgical instrument. The interventional 'target access' surgical endoscope is assisted by an external robotic device as part of the external computing platform. The external robot would help mitigate limitations of hand-eye coordination and able to perform rare ambidextrous surgical skills of a surgeon making complex manoeuvres possible.

6.0 Design concept of Rotitome-G

Rotitome-G is a high-resolution microsurgical endoscope with multiple integral assistive tools. It is a single portal endoscope concept to achieve the intraoperative goal of maximum resection of tumour tissue in constrained and unstructured spaces as tumour resection proceeds. The entire structure of the Rotitome-G is constructed on the principle of a semi-rigid compliant continuum robotic system. The maximum outer diameter of this compliant continuum endoscope is 5.5mm of varying length from 65mm or longer. It has two principal parts which are arranged concentrically. These are two co-axial outer and inner cylinders representing the trunk and the tendril respectively. The two tubular structures nested together have a common axis of rotation [Fig. 6].

The central tubular component is designed to either spin or have rotating protraction and retraction movements. The hosting external tube resembles the hollow muscular trunk of an elephant. The coaxial central tubular component is based on plant tendril, so called because it has a smaller diameter relative to the hosting trunk and has greater degree of manoeuvrability. The structure of the truncal wall is complex. The force-transmitting actuating system is extramural (not shown), outside the trunk within a shrink wrap to have maximum mechanical

advantage. The optoelectronic transmission wires, cables, fibre optics, etc. are intramural, within its wall, to serve as the assistive devices arranged circumferentially on the face of its distal end.

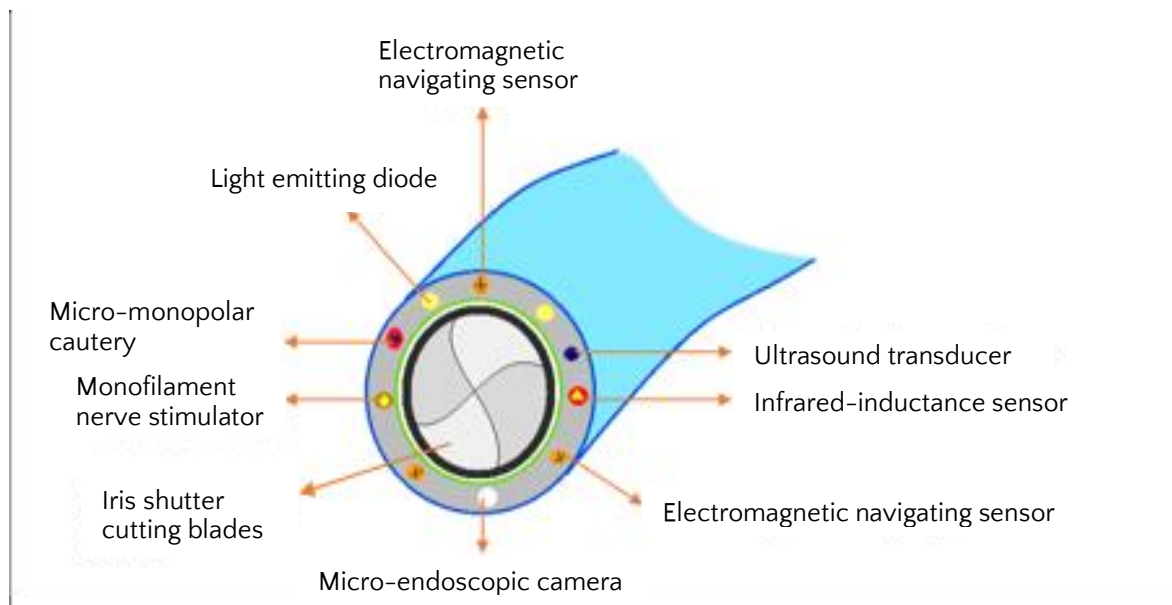
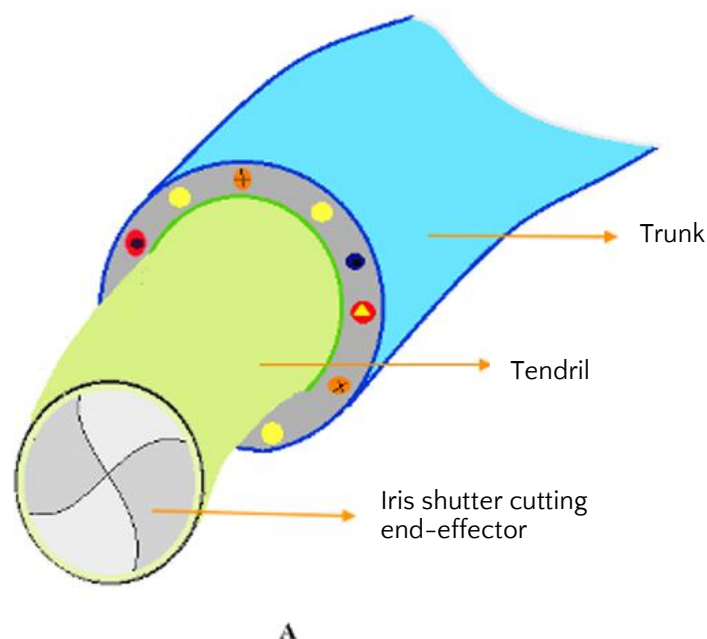


Figure 6. The co-axial concentric arrangement of the tubular trunk and the tendril is nested together.

The coaxial centrally placed tendril has a forward-cutting end. It comes in two versions serving as the sarcotome for the resection of tumour tissue [Fig. 7 A and B]. The cutting end of the Rotitome-G is designed based on the anatomy of the Rotifer’s corona and oral cavity to cut or abrade and simultaneously remove the tissue debris. The version designed like the coronal cilia is a high-speed rotary cutting sarcotome. It has circumferentially arranged multiple filaments made of the polymer material of suitable stiffness akin to the bristles of a motorized toothbrush to abrade the softened and necrosed tumour tissue. The second version has hard-wearing sub-millimetre 3-4 metallic blades made of tungsten or similar hard-wearing material arranged like the iris shutter mechanism of an old-fashioned camera or a shutter dome.

The entire structure of the trunk and coaxial tendril is made of flexible materials with controlled variable stiffness to bring versatility and stability to the working end. It allows segmental flexibility and the ability to hold desired position and posture of the cutting end during pixelwise and voxel size tissue resection. The movement of the



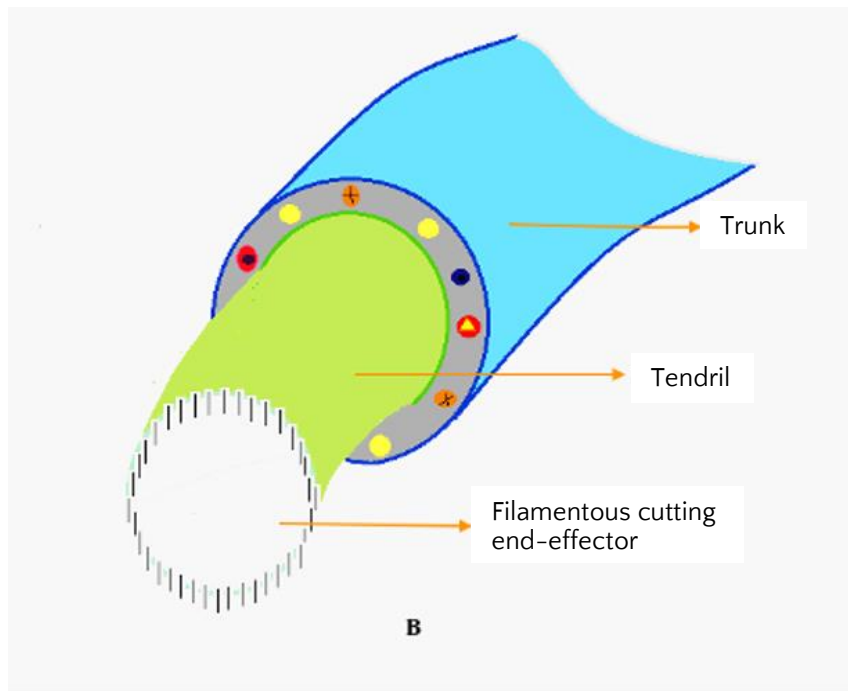


Figure 7. The two variations of Rotitome-G cutting heads **A.** Iris shutter and **B.** filamentous corona.

entire assembly of the instrument is controlled by the movements of the outer compliant continuous tubular trunk. However, the internal rotating tendril in its corridor carrying the cutting end can act as an independent unit. The tendril can be replaced with an alternative dedicated cutting device or other dedicated assistive devices such as a larger laser or ultrasound probe, if so needed.

6.1 Structure of the Trunk

The skeleton of the trunk is made up of a pair of concentrically placed continuous parallel springs along the whole length of the Rotitome-G endoscope, making it a double-walled flexible tube. It is a continuous structure without

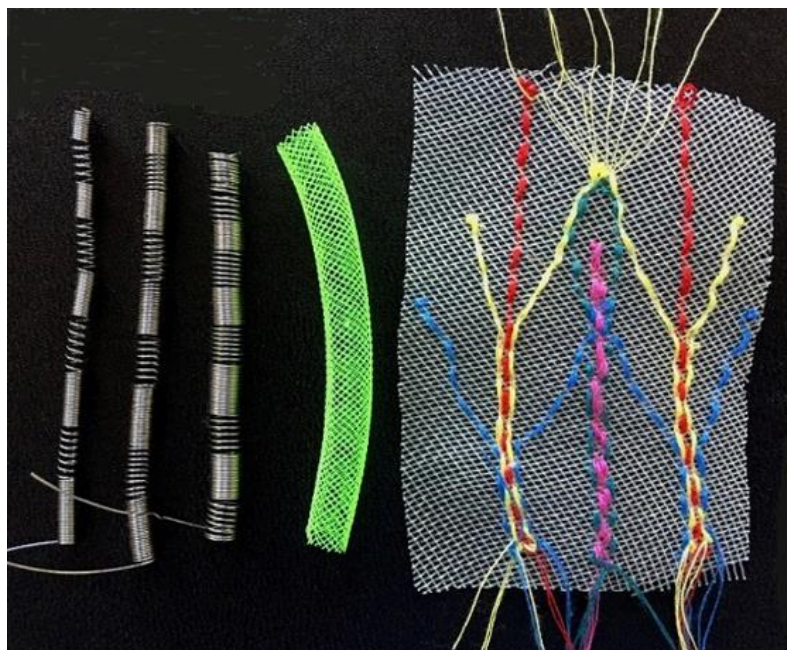


Figure 8. Illustration from left to right showing suggested design of the extension and compression springs in the continuum; tubular mesh sleeve acting as the Chinese finger trap to carry the embedded sliding actuator mechanism; and an exploded open view of the sleeve with embroidered extensor expansion arrangement.

true joints like the trunk of an elephant with an intramural arrangement of muscles embedded in its wall. Such that the musculocutaneous wall of the trunk can be divided into multiple segments to form pseudo-joints to bend at any point along its length and have infinite degrees of freedom to attain the desired pose of the end-effector. Similarly, the trunk of the Rotitome-G has a set of parallel pair of springs forming its wall having intramural space. Each spring in the continuum has an alternate arrangement of extension and compression spring segments at the same level. These segments are arranged in series like phalanges of a human finger with pseudo-joints [Fig. 8]. Each human finger has three phalanges arranged in series with true hinge joints. The phalanges successively have shorter lengths from the proximal to the distal end. Similarly, each extension spring segments representing the phalanges successively have shorter lengths from the proximal to the distal end of the trunk. However, the described structure of the instrument here has four or more phalanges, and a much longer most proximal phalanx called here as pre-phalanx (Pre-P) is the base phalanx equivalent to a metacarpal of the human hand. The compression spring segments in between the extension spring segments are also of variable lengths reducing in length from the proximal to the distal end.

The distal ends of the concentric parallel titanium springs forming the trunk are welded to a Titanium ring-shaped end-effector (not shown) to its inner and outer edges closing the intramural space distally for the optoelectronic components. The face of the ring carries the assistive devices as shown [Fig. 6]. The extramural space of the trunk has a mesh sleeve with an embedded/embroidered actuating system forming the extension-flexion expansion complex around the perimeter of the trunk within the shrink wrap made of a suitable flexible and extensile material to allow free movement of the trunk and the tendril. The proximal ends of the spring are managed appropriately depending on the design of the actuating system and other components moving the trunk.

An extended compliant continuum robotic system can have as many more phalanges as needed depending on the design and function of the system. The addition of each phalanx not only adds complexity to the structure and the actuating force transmission system, but also the mathematical algorithm, and the controlling platform.

The considered working length of the endoscope is sixty-five millimetres. The diameter of the outer trunk spring is 5.5 millimetres and that of the inner spring is 3.5mm. The reducing lengths of the phalanges (extension springs) including the pre-phalanx, from the proximal end, are 20mm, 10mm, 8mm, 6mm, and 5mm. The chosen lengths of the compression springs (interphalangeal pseudo-joints) from the distal to proximal end are 3mm, 3mm, 5mm, and 5mm. These numbers are arbitrary and can be different based on system functions. The entire continuous arrangements of flexible phalanges and pseudo-interphalangeal joints confer upon the structure possibility of an infinite degree of freedom. Nevertheless, given the restrictive stiffness of materials used, arrangement of the force transmitting actuating system, and constraints of unstructured working space may prove limiting factors.

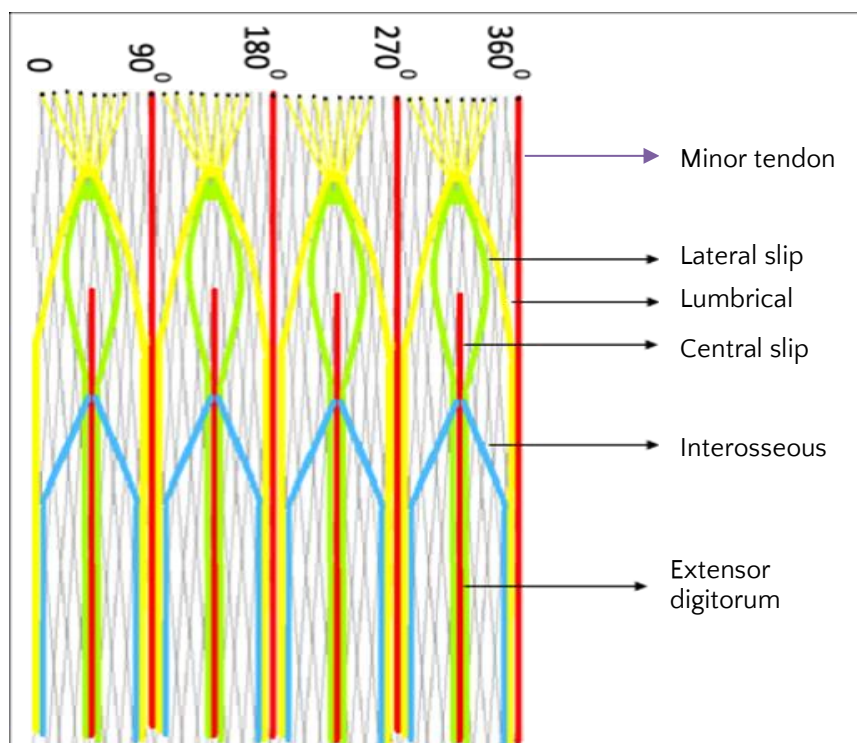


Figure 9. Illustration showing the arrangement of extension-flexion expansion weaved or embedded in the meshwork.

6.1.1 Actuating system of the trunk

The force-transmitting actuating system of the trunk is extramural on its external surface, to be at a maximum distance from the neutral axis of the endoscope body. The sliding arrangement of the force-transmitting sinews is very similar to the extensor tendon expansion of human fingers, but with a difference in the form of extension-flexion tendon expansion either embedded or weaved in the tubular Chinese finger grip meshwork [Fig. 8]. There are four such units distributed at 90 degrees to each other on the dorsal, ventral, and two lateral sides of the trunk. The four extension-flexion tendon expansions are distributed and distally inserted between 360 degrees to 0 degrees on the distal end-effector titanium ring [Fig. 9]. As there are four effective phalanges and a pre-phalanx, the structure of the extension-flexion tendon expansion unit can be modified accordingly, maintaining the natural principles of its function to bring about consensual movements of flexion and extension of various phalanges acting as agonists and antagonists to attain the required posture, stability, and position of the end-effector face normal to the tissue plane for resection. Each of the extension-flexion tendon expansion units has a central major tendon (extensor tendon) flanked by two minor tendons sharing with adjacent major tendons. The minor tendons insert directly at 90 degrees, 180 degrees, 270 degrees, and 0/360 degrees on the end-effector ring carrying the assistive devices. The central major tendon trifurcates so that the central slip is attached to the base of the phalanx equivalent to the middle phalanx of a finger, and the lateral slips travel further distally by-passing middle-level phalanx to take insertion on the base of the most distal phalanx. It splits into eight strands to finally attach to the perimeter of the end-effector ring. There are pairs of tendinous slips that connect the minor tendons to the central major tendon. The proximal pair of tendinous slips arise from the minor tendon to merge with the central major tendon at the level before it trifurcates. The second pair of tendinous slips merge with lateral slips of the trifurcated major tendon at the level to gain insertion distally before the two lateral slips fuse to insert into the base of the most distal phalanx. The rest of the extension-flexion tendon expansion sets follow the same pattern to complete the circumferential sleeve around the trunk in the extramural space. The meshwork sleeve of the Chinese finger grip that makes the support structure of the actuating extension-flexion tendon expansion is made of right-handed and left-handed helical strands for torsional movements in conjunction with flexion and extension. This integrated force-transmitting system confers additional strength, stability, and variable stiffness to the pose of the trunk and contained tendril.

6.1.2 Optics, and assistive instruments

The Rotitome-G is a flexible fibre optic instrument. To assist navigated surgical procedure through a single portal it includes a micro-endoscopic charged coupled device (CCD) camera or a higher version video system, two light emitting diodes, three electromagnetic navigating sensors, an ultrasonic micro-transducer, an infrared inductance transducer to assess tissue density by measuring beam deformation, monofilament nerve stimulator which sends current radially to cover greater brain tissue to locate eloquent tissues for neuro-monitoring, and a micro-monopolar cautery filament. These assistive devices are integrated into the face of the end-effector Titanium ring at the distal end of the trunk [Fig. 5]. The wires, cables, and fibre optics serving the assistive micro devices are intramural between the two concentrically placed parallel continuous springs of the trunk. Both the internal and external surfaces of the trunk are enclosed in suitable material without further affecting the compliance of the trunk. The role of the assistive devices is discussed in detail elsewhere (H. Gandhi, 2022).

An optical fibre has a diameter equivalent to human hair, by drawing silica glass or plastic (T. Brown, 2001). A bundle of tens or hundreds of fibres serves the dual purpose of illuminating an object and imaging. The optical fibres are enclosed in a transparent cladding of lower refractive index to cause the internal reflection acting as a mirror and waveguide. It produces intense illumination of the object and resolution depending upon the number of fibres in a bundle. A bundle of glass fibre is durable and has limited bending depending on the diameter of each fibre. A light ray transmitted through the core of a single fibre has a characteristic single path described as "mode," whereas a larger fibre transmitting a wave having multiple angles is called "multi-modes." The latter is cheaper, but the image quality is poor due to the dispersion of waves with several different angles and traveling different distances. The single mode fibre has an average core diameter of 9 micrometres, whereas multimode fibre has 50 to 62.5 micrometres or more. Single fibre imaging is free of distortion, has minimal attenuation, and is speedier. The cladding increases the diameter of a 9 micrometres single fibre to 125 micrometres (Jacobs I, 2001). There are single fibre optic imaging modalities, but for higher quality image acquisition it is preferable to have enough fibres in a bundle to form a ten-megapixel CCD camera (Grant et al., 2019). The images are magnified by intervening lenses and filters to enhance the image resolution. Rotitome -G has the provision of a wide-angle and very short focal length to view tissues at near direct contact.

6.2 Structure and Function of the Tendril

The tendril part of the Rotitome-G is the central coaxial cutting instrument. It has two variations based on the cutting-end design having completely different operative mechanisms. Fundamentally, the embodiment of the two is like the structure of the trunk except that the tendril has a single continuous spring rather than two parallel concentric springs. The spring embodiment has the matching length, but its diameter is 2.5 mm. The spring is segmented like the phalanges with interphalangeal pseudo-joints. The phalanges are constituted by extension

springs and interphalangeal segments made of compression springs corresponding to the trunk springs. The lengths of the segments of the tendril are the same as the trunk so that it conforms to the contour of the trunk. It follows the same path within the given space to a position perpendicular to the tissue plane getting ready to perform tissue resection. The core of the spring forms the lumen of the tendril acting as a channel to receive resected tissue, and function as a lavage and suction tube. During surgery, a dedicated submillimetre laser cutting device or additional electrocautery can be passed down without retrieving the tendril. Occasionally, the tendril may be removed and replaced with a larger befitting instrument.

One of the tendril variations is a high-speed rotary cutting instrument that operates concentric to the trunk. Its cutting head is akin to the circumferential arrangement of filaments like the corona of the Rotifer. The filaments are made of a stiff polymeric material, each bristle having specified diameter and length, such that it abrades or erodes the soft or necrosed tissues equivalent to desired voxel size volume. The diameter of the filamentous corona would be restricted by the maximum diameter of the tendril. As the softer pathological tissue is abraded or grazed the excised tissue is churned and liquified further. The deliquesced tissue is sucked continuously to clear the space ahead of the cutting end to maintain the visibility of the endoscope's microscopic wide-angle camera eye. The intermittent and continuous suction power must be controlled according to the density of the tissues to prevent sucking undesirable tissues inadvertently within unstructured and constrained anatomical spaces. The cutting end can be protracted and retracted to a limited depth of two to three voxels to prevent injuring the normal and eloquent tissues past the extent of pathology and the splattering of abraded tissues blocking the view.

The shaft of the second version of the tendril is like the former variation except for the cutting-end design. It is not designed to spin but rotate through part of its circumference within the trunk tunnel. The continuous spring embodiment has segments equivalent to that of the trunk to follow its contours. This tendril variation has a set of hard-wearing 3-4 metallic cutting blades like the chitinous teeth of the Rotifer arranged in the form of a high-speed leaf diaphragm shutter to bite and direct tissue debris into its lumen [Fig. 7A]. It is specifically designed to protract and retract with partial rotation to bite and release the pathological tissue. This is to prevent yanking of more than the desired number of pixels or voxels of the tumour tissue. At each bite, the cutting head rotates resecting the desired volume of tissue and breaking it at the correct depth cleanly before it gets swallowed into the lumen of the tendril and sucked proximally. It is designed to take one bite at a time abutting normal and eloquent structures during the excision of slender tumour extensions. With this version, the resection process of protraction to bite, retraction, and swallowing of the tissue can be slow but it would be precise.

The mechanical shutter cycle of opening, biting, and closing is controlled with the clicking of a computer mouse to complete each cycle instantaneously. In between each cycle, the new position of the cutting head is attained as planned or reposition with precise movement of the cursor and with click of the mouse button complete the next cycle taking a fresh bite and swallowing into the lumen. The pressing down and release of the mouse button also actuates the cocking mechanism to complete the shutter cycle of the cutting blades. It is followed by repositioning of the cutting head in the physical space equivalent to the next set of pixels/voxels of a lesion. The profile of the shutter diaphragm in a closed state is convex facing the tissue plane to get an easy pixel/voxel size to bite each time. Each blade has a rake angle at its cutting edge on its deep surface in the direction of its circumferential rotation. The cycle begins with protraction, to advance the cutting end to match the pixel/voxel in the image space and simultaneously to the corresponding area of the tissue in the physical space, taking a bite, rotating, and retracting at the same time cutting the tissue volume smoothly and 'swallow.' The helical protraction and retraction movement allow clean-cutting action. When the cutting face is normal to the tissue plane the captured blood vessel will likely have transversely cut edges. It will effectively cause the circular muscles to close the vessel opening evenly to achieve better haemostasis.

6.2.1 Actuating system of the tendril

The shaft of the high-speed spinning tendril version with filamentous corona is driven by a non-contact electromagnetic external motor. In the other version to protract and retract the cutting head of the tendril, there is a pair of sinews for transmitting the actuating force. They are extramural and enclosed in the skin of the tendril. They are oriented in opposing right- and left-handed helices to bring about torsional protraction and retraction movements of the distal cutting end in conjunction with compression and extension of the tendril. Once again, the strap-shaped sinews of appropriate width are made of non-extensile flexible silk material carrying the required sensors. The electromechanical device for driving the shutter diaphragm is placed in such a way that it does not obstruct movements of the tendril and the flow of the debris collected during tissue pikelectomy.

The trunk and the tendril have multiple degrees of freedom in coronal and sagittal planes of the physical space. The steerable cutting end can sweep and graze the pathological lesion perpendicular to the tissue plane as the excision proceeds. The trunk and the tendril of the Rotitome-G can be retroflexed as a unit, and the tendril can be rotated freely within the trunk. The tendril can be protracted to a required length independent of the trunk to access the ceiling of a tumour cavity proximally.

7.0 Surgical implementation of Rotitome-G

The *target access* single portal Rotitome-G with its two variations of cutting mechanisms resecting tissues equivalent to pixel size area or voxel size volume is a newly conceptualized endoscopic function. The procedure demands intensive patient-specific pre-surgical planning, MRI imaging, 3D image reconstruction of the tumour, segmentation of the tumour and contiguous eloquent structures; finite element modelling and analysis to know the density distribution of the tumour tissue. It engages an interdisciplinary team of surgeons, radiologists, and neurologists in collaboration with a clinical biomechanical engineer. The process of tissue resection in the tumour space is actuated pixel-by-pixel in the image space under computer navigation. The path of the Rotitome-G trunk and the tendril is pre-planned in addition to the programming of an external rigid robotic system in the non-sterile area to automatically reposition the leading end of the Rotitome-G in the tumour space in all the planes. Thus, there are several technical and surgical issues to optimize its multiple functions.

The integral functional design of the Rotitome-G includes sensing, actuating, and control systems for feedback and response of its trunk and tendril as the tumour resection proceeds in the image space. The corresponding progress of tumour resection is updated either with the integral ultrasound probe or intra-operative MRI at regular intervals to prevent inadvertent injury to normal tissues due to collapse of the tumour cavity and brain-shift (Gerard et al., 2017; Hartkens et al., 2003). It is preferable to make available a 3D stereo tessellation lithographic (STL) model of the tumour and adjacent normal structure for tumour resection simulation preoperatively. It will also help establish the path planning of the leading end of the Rotitome-G, know the likely size of the evolving tumour cavity and brain shift during a surgical procedure and at the end of it.

In *target access surgery*, the specific anatomy of an intracranial tumour accessed through a burr-hole aperture is targeted under image guidance and navigation. MRI is the preferred preoperative and intraoperative imaging modality because it is free of radiation and show better tissue contrast than CT. The eloquent brain structures can be seen with greater clarity, and the tracts can be better defined with MRI diffusion tensor imaging. A baseline segmentation of the lesion and surrounding normal brain structures during preoperative planning provide an opportunity to undertake image registration to measure tumour mass reduction and brain shift with intraoperative MRI or ultrasound imaging (Carton et al., 2020; Nakaji & Spetzler, 2004). The included micro-machined ultrasonic transducer technology in Rotitome-G can deliver real-time 3D imaging during surgery (Khuri-Yakub & Oralkan, 2011). For navigation, Rotitome-G has miniature sensor coils (Aurora® Northern Digital Inc. and the 3D Guidance med SAFE TM, Ascension Technology Corp. Burlington, VT) embedded intramurally in its trunk for the location of the cutting end with six degrees of freedom in the tumour space corresponding to the image space at pixel level. The electromagnetic navigation sensors are designed to automatically co-register the neuronavigation system to follow intraoperative updates. As the navigation system and imaging is based on electromagnetism all the instruments should be made of non-ferrous material.

After a patient's head is rigidly fixed in the most desirable position the regional anatomy and region of interest (physical space/tumour space) are co-registered to virtual image anatomy (image space). The pathological lesion should be isocentric with the MRI gantry if such a facility is available, which makes correspondence of the physical space and image space much easier. Following skin preparation at the targeted site, a 15mm diameter hole craniotomy is made. The dura is incised making a cruciate incision in advance and bleeders are cauterized. The specially designed Titanium watertight cranial portal device (CPD) described elsewhere (H. Gandhi, 2022) is screwed into the craniotomy portal engaging both the tables of the skull. The plug of the CPD is removed and the diaphragm of the CPD is opened by making a cruciate incision no larger than 5.0 mm diameter to insert the Rotitome-G cannula held snugly in it. A trans-sulcus approach is preferable wherever possible. The graded navigable blunt trocars are used to develop a safe trajectory for the *target access* surgical track to reach the superficial surface of the lesion. Upon reaching the correct size dedicated operating cannula accompanying the final trocar is passed. The trocar is removed, and the cannula is screwed onto the CPD socket ring in a stable position. The trunk of the Rotitome-G is lowered to reach the surface of the tumour and held in position with an external rigid arm robotic system.

All the assistive tools are checked, and the physical space is corresponded to the image space, before one of the two tendrils with suitable cutting head is lowered. The image space is zoomed-in to pixel level as per preoperative planning. Then the leading end-effector of the Rotitome-G is corresponded to the image space before actuating the cutting head. The cutting head is actuated with a handheld cursor locator device such as a computer mouse. The response in the physical or tumour space corresponds to the pixel-erasing action of the cursor in the image space on the visual display unit. The protraction of the tendril head, nipping off the tumour tissue by the diaphragm shutter cutting tool, rotation, and retraction occurs in response to the stimulus generated by the mouse button. The pixel-by-pixel resection to a voxel depth is preferred for more peripheral parts of the lesion and tumour tissue insinuating between normal structures and eloquent tissues. For improved safety, the action is executed after the application of the monofilament nerve stimulator, real-time ultrasound, and cellular level magnification to confirm the location of the correct pixel.

The alternative version of the high-speed spinning abradar is preferred for centrally necrosed and softer tumour material as judged based on tissue density after checking with the provided non-tactile infrared inductance device

or based on pre-operative tissue segmentation and density assessment (H. S. Gandhi, 2022). The heterogeneous distribution of tissue density is preferably mapped, and colour coded preoperatively for ease and to save surgical time. The flexible compliant continuum design of the trunk and the tendril move together following the pre-programmed pathway. However, the abrading tendril can be extended independent of the hosting trunk as required within constraints of the tumour cavity. The diaphragm shutter cutting tool can also move independent of the trunk to only a limited length beyond set protraction and retraction. When there is adequate tumour cavity formation the tendril head can be steered in all possible degrees of freedom to sweep and graze the pixel plain in the image space and tumour space to remove the corresponding tumour tissue rapidly. The entire path must be pre-planned based on the shape, size, and orientation of the tumour mass to the eloquent tissues. Similarly, to speed up the task, the knowledge of the density distribution of the tumour tissue in advance would help in selecting one of the two versions for the task.

The compliant structure of the Rotitome-G allows retroflexion of the trunk and the tendril to reach out proximal zones, the ceiling of the tumour cavity, where the resection process is initiated. It is best to leave the proximal zones towards the end so that there is enough room for manoeuvring the trunk and steering the tendril reaching out to all the hard-to-reach places. The tumour areas are classified, and the path of the tool is defined pre-operatively. The tumour cavity is kept distended with fluid analogous to the tonicity of the cerebrospinal fluid continuously to lavage the cavity. It will prevent further brain shift and maintain a clear view. As well as to cause tamponade of haemorrhagic ooze. The central aspirating lumen of the tendril is actuated at the same time the cutting head takes a bite at the optimum vacuum pressure. To lavage and distend the tumour cavity the lumen is connected to hyperosmotic or isotonic fluid delivered under gravity via an operator-controlled two-way stopcock valve system sharing the suction channel.

The rhizomatous extensions of the tumour tissues are reached by manoeuvring the tendril independent of the trunk following one pixel at a time equal to voxel volume head-on in image space avoiding the eloquent tissues. The visibility of the tumour tissue may be enhanced by applying one of the prevalent compatible tumour stains, such as 5-Amino-Levulinic Acid, corresponding the image pixels and stained tissues. The surgeon may attempt a graded approach by biting at the residual tumour tissues based on experience by overriding the built-in feedback mechanism to control the path of the cutting head as planned preoperatively. A surgically relevant segmentation of the tumour tissue and that of eloquent tissues, and density distribution in 3D is crucial during path planning of the cutting head. In the 'difficult' scenario it is best to consider patient-specific finite element modelling and analysis, and simulation of the procedure on a true-to-life 3D printed model. The same STL files can be applied intraoperatively after considering any changes that may occur due to brain shift and collapse of the enlarging tumour cavity.

It is good to remember that no tumour is uniformly round as often illustrated. A hypothetical path planning is

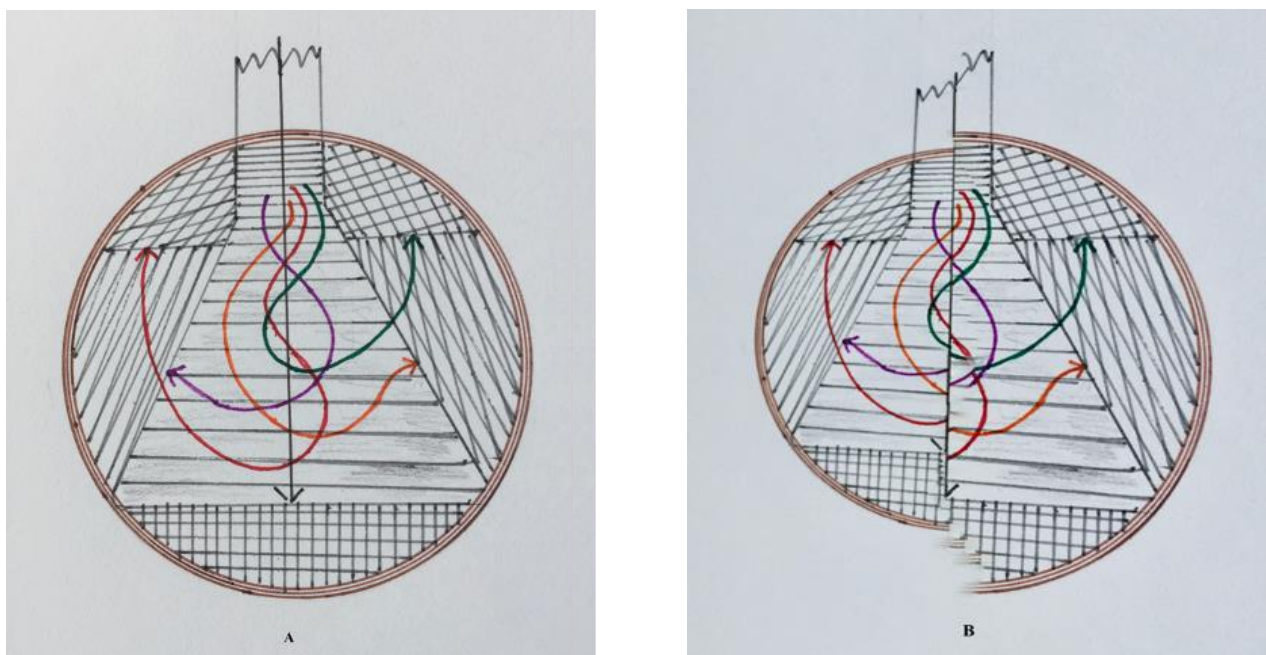


Figure 10. Classification of the tumour segments by hatch-marking or colour coding and suggested paths leading to the development of a conical flask-shaped tumour cavity.

suggested here to develop a tumour cavity in the form of a round bottom or a flat bottom conical flask [Fig. 10]. This can take any other similar outline in a 2D image slice depending on the 3D shape and size of a solid tumour. The proximal part will always have a straight neck-shaped path because of the fixed entry cannula for Rotitome-G. The resection begins at the tumour surface and widens as more room is available for greater freedom of trunk-tendril movement within the developing tumour cavity. Despite the preoperative plan, it will be prudent of the interdisciplinary team to update the anatomy of the tumour with frequent image segmentation and registration intraoperatively to have the best use of the micro-ultrasound transducer of Rotitome-G. The surgical versatility of Rotitome-G is designed to extend to a rigid robotic system outside the sterile region through a common computing platform. The rigid ²robot system can be an honest serf at the command of the operating surgeon to take over the operations of the Rotitome-G at the final frontier of tumour tissue removal based on experience and knowledge of eloquent tissue bit by bit. There is no surgical robot that has enough versatility to match the upper extremity kinematics of a well-trained surgeon with more than 24 degrees of freedom (Motkoski & Sutherland, 2014).

8.0 Coordinated path planning

Rotitome-G is continuum-compliant robot having several continuous segments of extension and compression springs. It has flexible joints to allow multiple degrees of freedom, and capabilities following desired contours within a constrained and unstructured space. A modular design with exchangeable components would help make suitable choices expanding its applications and increasing its adaptability to the single aperture 'target access surgery.' The fundamental objective for a path planner is the coordination of the patient's physical space and image space. Therefore, the path planner must have a thorough knowledge of pathological anatomy and normal adjacent anatomy to plan the trajectory of Rotitome-G's cutting head.

For complete resection of a brain tumour, including its rhizoid extensions flawless presurgical path planning is extremely important. Therefore, at the time of image segmentation of the tumour, the adjacent normal anatomy is also segmented, with particular attention to the eloquent structures. To achieve this none of the images included for segmentation should undergo a smoothing process or any such alteration to enhance image properties. It would crop many peripheral voxels forming the extensions of the tumour in its 3D segmentation map at the boundary of the tumour leaving residual tumour tissue behind. The path tracing of the end-effector begins at the craniotomy aperture to reach the surface of the tumour in the physical space and pixels in the image space. The path ends once it has covered the entire tumour volume to its last voxel. The pathological anatomy is never identical in size, shape, and consistency occupying the same anatomical space in every patient. It never remains the same as the resection proceeds with the formation of variable shape tumour cavities. Therefore, for patient-specific tumour management, the path planner must construct an offline plan for simulating the complete excision of the patient's tumour on a 3D virtual model, in the company of the most responsible surgeon. Only then a rectified plan is constructed protecting relevant vascular and eloquent tissue as obstacles, tumour cavity evolution, and brain shift. It could also mean active engagement of the planner to progressively construct an online plan modification based on sensor data update used in a feedback loop, MRI, real-time ultrasound, infra-red inductance transducer, and monofilament neural monitoring findings.

8.1 Principles of path planning

The process of planning the movements of a robotic system can be challenging in tumour surgery as it involves a more complex pathway than articulated segments of a train on a linear structured track without obstacles. In neurosurgery, the objective is complete removal of an intracranial pathological lesion in an unstructured constrained space that is evolving at each bite of the tissue. At the same time, protecting important neurovascular structures and normal adjacent anatomy. The task is to create a safe obstacle-free patient-specific path for the end-effector and proximal endoscopic trunk, from one configuration to another as would be for any robot (Howie C et al., 2005). Each new patient with a distinctive tumour and distorted intracranial anatomical space configuration must be addressed with an individual mathematical solution to the corresponding image space at surgery, from beginning to end. A configuration is a set of working angular positions of the robot to attain the optimal position and orientation of the end-effector in progressively changing physical space (configuration space) (Howie C et al., 2005). This is the reason that it is important to have the experience at the time of the pre-surgical simulation.

The basic design of all robotic systems is entirely based on the human upper extremity to reach out precisely and grasp the target object. Most systems have two bone segments (upper arm and forearm) with the elbow joint, wrist, and hand as the end-effector organ. It is a top-down design for forward kinematics, where the operator takes control of the end-effector by rotating one or more bone segments at the joint axis to position the end-effector. Contrarily, currently the robotic systems are programmed for what is called inverse kinematics, which is bottom-up design. In inverse kinematics, all the joint axes are activated to hold the desired position of the end-effector. For example, in the gaming and film industry during the stance phase of the gait cycle, the foot and hip

² A mechanical device that does some of the work of human beings, to take over dull mechanical activities. The term invented by Karel Capek (1890-1938), a Czech writer for his play, *R.U.R.*; from Czech *robota* work, *Robotnik* serf.

joint axis are fixed in position, while the joint axes of the ankle and knee are stabilized by resolving variable angles at these joints to follow a particular path with the help of complex computer vision and mathematics. Similarly, in the case of a compliant robotic system, the kinematic chain is programmed by kinematic equations to command the motion of the entire structure for the end-effector to reach and operate at the desired target. In forward kinematics, the joint angles decide the posture and position of the end-effector, and in inverse kinematics, the posture and the position of the end-effector are effectively held in place finally by attained variable joint angles. This is not a trivial task to compute when planning a path for a compliant robot with more than two segments and joints. In a surgical scenario, such as intracranial tumour resection, no single kinematic solution may be optimal. It deserves a combination of kinematic equations to compute the tumour resection pathway as a part of the presurgical planning. Preferably, in the form of simulation on an STL tumour model, finite element modelling, and analysis to avoid surprises during surgery. The team must be prepared to make necessary changes to manage as the tumour cavity enlarges with the corresponding brain shift.

Path or trajectory planning is an important part of the robotic function executed by higher-level computer programming. In a constrained evolving space, the key is to develop an obstacle-free straight or curved path [Figure 10]. A robotic endoscope must attain a new configuration as it progresses from one voxel layer to the next to operate in a different dimension altogether. All surgical procedures are bound by time limitations for patient health and time cost. The surgeon can exploit the omnidirectional capabilities of the Rotitome-G. It is a semi-automatic instrument for manual intervention of the supervising surgeon where the path is continually being replanned online. The ultrasound sensor can help reposition the cutting end itself updated by calculating the physical space, as well as refreshing its configuration to updated image space. In 3D physical space, with the development of new obstacles, the remapping endeavour can be challenging. Under such circumstances, the complex path and coverage can only be resolved by having a simultaneous localization and mapping facility for coverage of the space safely, systematically, and effectively (Howie C et al., 2005). The coverage of the entire tumour physical space or configuration space is undertaken by sensory scanning pixel-by-pixel in the image space for the complete tumour resection. The sweeping and grazing motion of the cutting end of Rotitome-G for space coverage is like a floor-sweeping robot, a lawnmower grazing robot, or a paint-spraying gliding robot. But with a difference that Rotitome-G is faced with hundreds of voxel layers to graze.

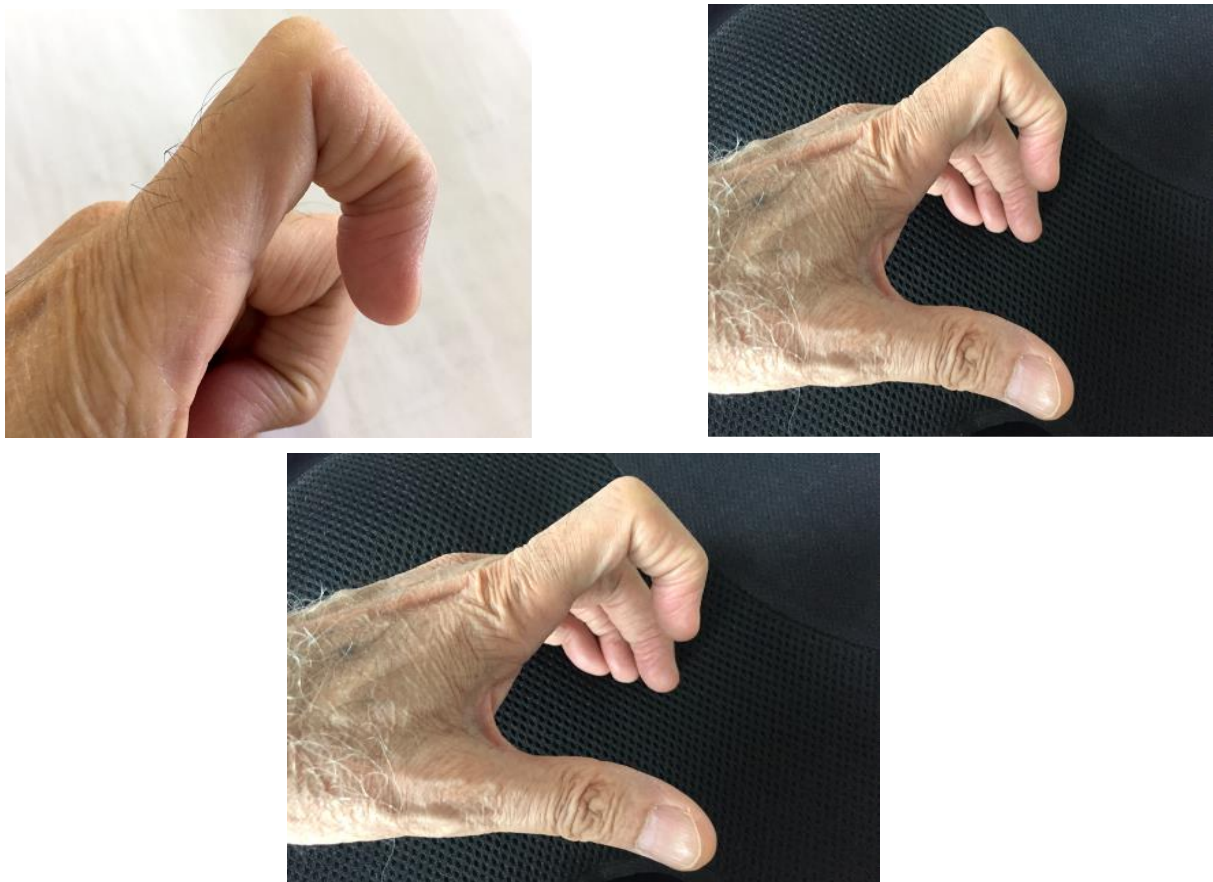


Figure 11. Combination of complex flexion, extension, and sideways adduction movements at the metacarpophalangeal and interphalangeal joints of the index finger of the left hand.

In summary, path planning is dependent upon the degree of freedom of the robotic system and the physical space constraints. The task of the robotic endoscope is to 1) navigate around obstacles from one configuration to the next; 2) coverage of the entire space by sensory or real-time ultrasound imaging to have the pixel-by-pixel correspondence of the physical space updated to image space; 3) localization of self-status by using the map; 4) remapping the evolving physical space or getting updated to the fresh image space by either real-time ultrasound or MRI. Further discussion of robot motion and how to develop mathematical algorithms is beyond the scope of this article.

8.2 Versatile kinematic template of coordination of finger movements applied to path planning of Rotitome-G

The successful outcome of path planning is dependent on the degree of freedom and coordinated movements of the cutting end of the Rotitome-G and its proximal segments within the physical space. It is the coordination of the finger, hand, and wrist joints that the interphalangeal and metacarpophalangeal joints flex and extend simultaneously. As the design of this semi-rigid compliant continuum endoscope robot is inspired by the anatomy and kinematics of the muscular hydrostat and human finger the function of Rotitome-G can be explained by coordination of flexion-extension of IP and MCP joints and limited rotation at the MCP joint required to sweep and graze tumour tissue [Fig. 11].

The complex posturing of the finger is due to the simultaneous contraction of several individual muscles in the hand and forearm. The muscles move all those joints across which their tendon passes perpendicular to their axis of rotation to position the phalanges arranged in a chain by measured proportions in tandem for the desired task. The eccentric contraction of the antagonistic muscles assists to generate variable stiffness to maintain the position and posture to carry out the task. The force of the turning moment with which each joint moves depends on the distance of the tendon from the longitudinal central axis of the phalanges. Greater the distance greater will be the turning effect but the range of motion will be proportionately smaller (Standring, 2008). A balanced contraction of the extensor tendon expansion, finger flexors, lumbricals, and interossei acting on the extensor tendon expansion can bring a finger into a variety of postures in a steady position. Equivalent movements and postures can be attained by Rotitome-G following the planned path for the resection of a tumour.

The process of path planning, algorithm, implementation, and forces acting on the tissues can be extremely sophisticated trying to prevent crushing the tissues during cutting and retraction of the cutting end with optimal torque. A hypothetical path of Rotitome-G is shown [Fig. 12].

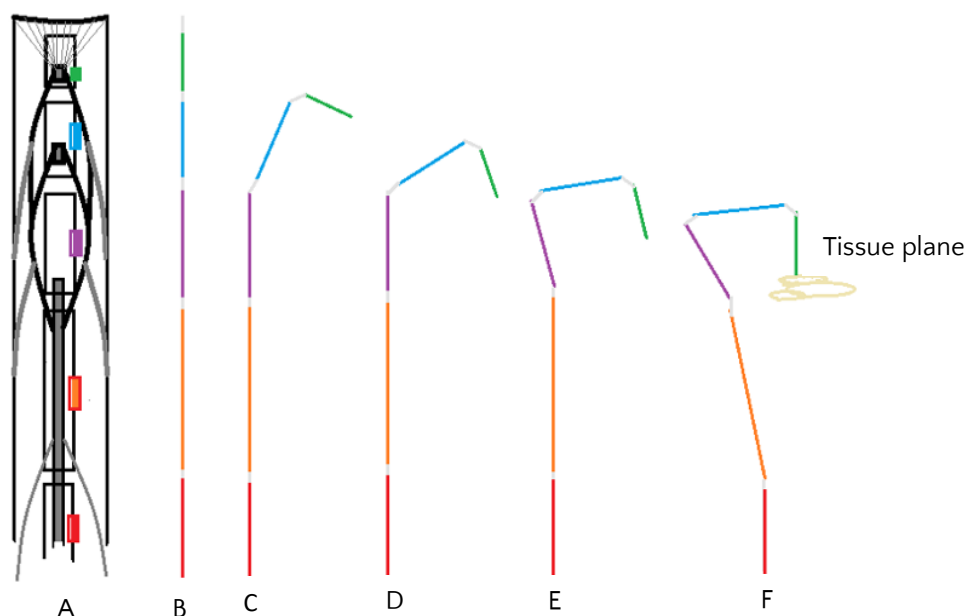


Figure 12. From left to right, A, a line drawing of the extensor expansion complex and B to F, a simplified path showing the progressive flexion and extension pose of various phalangeal segments in series to bring the end-effector normal to the tissue plane.

9.0 Comments

The most important functional components of an endoscopic instrument are its camera and fibre optic bundle. The knowledge of wider applications of fibre optics may be recent, but the phenomena of guiding light and bending the rays in a medium of a higher refractive index have been known since the 1840s. It was first noted by Swiss physicist Daniel Colladon that light could be shone through a column of water due to internal reflection. However,

it was not until 1954 that Narinder Singh Kapany demonstrated experimentally in a bundle of glass fibres as a Ph.D. student in the laboratory of Harold Hopkins at the Imperial College, London, and published the results (Hopkins H & Kapany NS, 1954; J.Hecht, 2004). It was Kapany, who coined the term “fibre optic” in 1966 describing the characteristics of the glass fibre in *Scientific American*. In 1967, Karl Storz, Tutillingham, Germany, adopted them for relatively much higher light illuminating strength compared to rigid glass rod endoscopes for constructing flexible endoscopes. Optical fibre also collects and transmits image data with an additional image-enhancing set of lenses. Secondly, the development of materials in the fabrication of optical fibre, particularly at low-cost and low-temperature polymers with additional flexibility makes them attractive for large core and short-distance applications to increase illumination (T. Brown, 2001). Fibre optic technology is advancing towards endoscopes without the lens for biosensing and imaging using hollow-core photonic crystal fibres and multicore and multimode fibres combined with wavefront shaping for flexible nonlinear imaging endoscopes and Raman probes (Rigneault et al., 2018). The nonlinear flexible endoscope and Raman probes have demonstrated deep brain neuron network activity in living mice and deep tissue morphology.

The fibre optic light transmission system, flexible actuators, and sensors have made the conception of compliant design of the Rotitome-G possible to function in an unstructured and constrained surgical environment. The functional necessity to have an excessive degree of freedom in the animal world than commonly required has allowed the inclusion of a well-known redundancy concept in robotic systems. The redundancy in biology is a pre-emptive tactical principle in reserve to enhance performance normally and under emergent circumstances.



Figure 13. Elongated body in a worm demonstrating hyper-redundancy (Modified image, acquired from public domain).

Similarly, the redundancy in robots means that it has a greater number of functional degrees of freedom for improved performance. When a structure has manifold or infinite functional degrees of freedom to increase its mechanical performance than is normally required, it is referred to as hyper-redundancy [Fig. 13]. The hyper-redundancy design feature in robots (Chirikjian GS, 1992) and that of the Rotitome-G are analogous to the extensile long bodies of the worms and arthropods; proboscis and tentacles; prehensile tails for balancing; long tongues and tendrils for grasping and twirling. All these organs have specifically evolved for feeding, fending, locomotion, and many more purposes. It means in nature nothing is redundant, making these biological structural evolutions ‘obligatory redundancies’, necessitated by the functional demands of a subject. On the other hand, in the case of robots and Rotitome -G, the introduction of ‘facultative redundancy’ in their design can enable greater functional resolution, though optional, but elective by the necessity of tumour anatomy to compute patient-specific programming preoperatively and during the intraoperative update.

The significance and surgical relevance of including hyper-redundancy in Rotitome-G are to meet the patient-specific and variable path planning and better system control. It will allow a manifold degree of freedom to reconfigure the end-effector segment of the instrument during surgery. In addition, redundancy increases structural robustness and fracture prevention of its components, and avoidance of obstacles such as major blood vessels and escaping eloquent tracts discovered on MRI updates, reprogramming of the end-effector configuration. Thereby, increasing safety and mitigation of experienced hazards during the learning phase.

As in the case of the human upper extremity under the control of the central and peripheral nervous system, the forward kinematic design provides only one solution to reach a specified target through rotation at the joint axes.

Whereas inverse kinematic motion provides several solutions to pose the end-effector by adapting the joint angles of the kinematic chain in evolving configuration space. As the end-effector moves to the next station, in the case of the Rotitome-G to the next pixel or voxel layer of the tumour the rest of the kinematic chain automatically adapts to the new posture. The new position and relative orientation of the phalangeal segments hold the pose of the end-effector. With the inclusion of hyper-redundancy, the applications of Rotitome-G widen to perform in the highly constrained surgical environment. It can be programmed to attain a fresh pose and adapt to a greater degree of freedom in emergent situations to circumvent unexpected difficulties.

The design and function of the Rotitome-G microsurgical endoscope are quite challenging because it comes not only with a camera, a fibre optic bundle, and various channels, but it has several assistive devices to accomplish a surgical procedure. The Rotitome-G has sub-centimetre main components from less than 2.5mm to 5.5mm and submillimetre inclusions. Before it can reach its full potential further work must be done to fulfil many practical challenges. Primarily, it is based on the upcoming technology of a compliant continuum robotic system, which is still under development. Secondly, it is not designed for pushing, pulling, creeping, grasping, or lifting purposes. Nor simply for exploration of environmental spaces, an inspection of biological structures, and inspect closed tubular anatomy of an organ for procuring diagnostic biopsies and therapies like haemostasis, passing ligatures, polypectomy, etc. The key challenges facing Rotitome-G are the miniaturized continuous structure of the trunk akin to a muscular hydrostat of an elephant trunk with the operational design equal to a new-born baby-sized little finger. Then there is the tendril although from the plant kingdom but follows the phalangeal anatomy of a finger. Like crossing one finger over the adjacent finger, the tendril has a unique progressive motion of circumnutation, which may find a role in certain surgical procedures. The trunk and the concentrically placed coaxial tendril are moved with intricate anatomy of the extensor tendon expansion of a human finger, unlike 3-4 separate strings acting like tendons in a robotic system. In the Rotitome-G there are two pairs of extension-flexion tendon expansions embedded or embroidered in the tubular Chinese finger grip mesh unique to its design. The opposing tendon expansion complexes acting as extensors and flexors co-ordinates agonistic and antagonistic movements, with some degree of torsion and possibly twirling motion of circumnutation, which is new to the soft compliant continuum robotic systems.

In compliant continuum robotic systems, the functional sub-millimetres, and nano-size modules such as carbon nanotube sensors for response and feedback tagged to the force transmitters are integral to their architecture. Therefore, several actuating technologies, sensors, and materials have been briefly reviewed to compose the operational structure of Rotitome-G. Many other considerations can be explored to select the best materials to optimally fulfil its design and functional challenges. The key materials of concern are to meet the requirements of non-ferrous elements to construct the continuous spring phalangeal system, actuation techniques for traction force transmission, and miniaturization of the actuating driving system. The newly conceived knitting of the extension-flexion tendon expansions integrated into the Chinese finger grip tubular mesh can be inspiring. The inclusion of fluidic pneumatic actuators and shape memory material actuators that need a change of temperature has been intentionally avoided to prevent inadvertent harm to the patient in busy and constrained anatomical spaces, such as the cranium, albeit similar concerns do exist over the safety of other anatomical sites. Elastomers are a reasonable alternative to spider silk as a material for transmitting actuating forces in a compliant continuum system, however, due to nonlinear elastic behaviour (Chen et al., 2020) like skin may be unsuitable to confer variable stiffness along a convoluted path and stability of the cutting end after many cycles. Given the design function of the tendon-driven architecture of Rotitome-G instead of integral pneumatic, chemical, temperature stimulated, or electrical actuation the current thought favours a motor-driven mechanism for rotation and translation of its parts and cutting end.

Among the two cutting heads mimicking the chitinous teeth of Rotifer as 3-4 blades arranged in the form of a shutter diaphragm may come with technical challenges. Instead resolving with intricate micro-machining skills, the currently prevalent 3D printing may not provide a very sharp and efficient cutting edge and rake angle to the blades. Apart from frequent stresses on the actuating transmission material, the cutting elements will bite into the varying density of the tumour tissues hundreds and thousands of times during a single operation and may require replacement. Therefore, it would be preferable to have a modular head design to easily exchange the cutting heads rather than being integral to the tendril. To this end, instead of a shutter diaphragm arrangement, the blades may be made to slide like the opening and closing of a dome.

Given the complex architecture of Rotitome-G, the controlling mathematical algorithms can be complex to make the instrument operate safely, efficiently, and reproducibly for inter-operator and intra-operator consistency; to make it user-friendly. For planning the path of the Rotitome-G's cutting end an accurate coupling algorithm between sensory feedback and the actuating system is needed for the movements of the trunk and tendril in the physical space corresponding to the image space during resection to safely accomplish maximum resection. Sooner or later there will be growing interest to bring together greater automation including artificial intelligence and speed in terms of timesaving. Otherwise, the mathematical algorithm and control programming of soft and compliant continuum robotic systems is not hugely different from the traditional rigid robots. An additional role of traditional rigid robot complimenting Rotitome-G requires experimental cadaveric and high-quality surgical

reporting. The functional fulfilment of the Rotitome-G will come with further development of compatible new materials based on the strength, non-extensibility, flexibility, optimal Young's modulus, viscoelasticity, virtually infinite degrees of freedom, fracture resistance and lifetime wear quality materials.

The limitations of the study are that the article has described the theoretically driven concept of an experimental microsurgical endoscope. It requires practical verification of its claimed functional capabilities through cadaveric experiments followed by clinical experience.

10.0 Conclusion

In conclusion, the envisioned advantage of Rotitome-G is that it is a *target access* single portal endoscopic sarcotome. It has several assistive devices integral to its design. The most prominent feature is the coupling of the compliant continuum trunk and a co-axial concentrically running tendril cutting tool to be able to resect pathological tissue at pixel/voxel level (*pixelectomy*). Certainly, like any new development cost-effectiveness in terms of surgical success is the completeness of tumour resection, low complication rate, and timesaving are the top priorities when introducing a new technology in patient care. Currently, there is neither surgical standardization nor unchallenged evidence in favour of robot-based surgical procedures. It can be difficult, but not impossible to raise a new complex single portal instrument, such as Rotitome-G based on the compliant continuum robotic system technology, which is still in its developing phase.

Declaration: This is to declares that design and construction of Rotitome-G microsurgical endoscope and application of the assistive instruments are intellectual properties of Dr. Harjeet Singh Gandhi.

Conflict of interest: The author declares that there is no conflict of interest.

Acknowledgement: The author would like to thank George Boyes of Biomedical Engineering workshop, Hamilton Health Sciences, Hamilton, Canada, for manufacturing the springs.

Funding: The author received no financial support for the research, authorship, and publication of this article.

References

- Abbott, R. (2004). History of neuroendoscopy. In *Neurosurgery Clinics of North America* (Vol. 15, Issue 1). [https://doi.org/10.1016/S1042-3680\(03\)00065-2](https://doi.org/10.1016/S1042-3680(03)00065-2)
- Abolfotoh, M., Bi, W. L., Hong, C. K., Almefty, K. K., Boskovitz, A., Dunn, I. F., & Al-Mefty, O. (2015). The combined microscopic-endoscopic technique for radical resection of cerebellopontine angle tumors. *Journal of Neurosurgery*, 123(5). <https://doi.org/10.3171/2014.10.JNS141465>
- Ainger, R., & Gillquist, J. (n.d.). *Arthroscopy of the knee*. Thieme Medical Publishers, New York.
- Alqahtani, A. A., Dallan, I., & Castelnovo, P. (2014). Transorbital Transnasal Endoscopic Combined Approach to Anterior and Middle Skull Base: Laboratory Investigation. *Otolaryngology-Head and Neck Surgery*, 151(1-suppl). <https://doi.org/10.1177/0194599814541627a316>
- Alqumsan, A. A., Khoo, S., & Norton, M. (2019). Robust control of continuum robots using Cosserat rod theory. *Mechanism and Machine Theory*, 131. <https://doi.org/10.1016/j.mechmachtheory.2018.09.011>
- Aylmore, H., Dimitrakakis, E., Carmichael, J., Khan, D., Stoyanov, D., Dorward, N., & Marcus, H. (2022). Specialised Surgical Instruments for Endoscopic and Endoscope-Assisted Neurosurgery: A Systematic Review of Safety, Efficacy and Usability. *Cancers*, 14(12), 1–20.
- Barber, S. M., Rangel-Castilla, L., & Baskin, D. (2013). Neuroendoscopic resection of intraventricular tumors: A systematic outcomes analysis. In *Minimally Invasive Surgery* (Vol. 2013). <https://doi.org/10.1155/2013/898753>
- Barth, O. (2000). Harmonic piezodrives - miniaturized servo motor. *Mechatronics*, 10(4). [https://doi.org/10.1016/S0957-4158\(99\)00062-8](https://doi.org/10.1016/S0957-4158(99)00062-8)
- Bhattu, A. A., & Kulkarni, S. (2021). Dynamics of Tendon Actuated Continuum Robots by Cosserat Rod Theory. In *CISM International Centre for Mechanical Sciences, Courses and Lectures* (Vol. 601). https://doi.org/10.1007/978-3-030-58380-4_50
- Brown, A. H. (1993). Circumnutations: From Darwin to space flights. In *Plant Physiology* (Vol. 101, Issue 2). <https://doi.org/10.1104/pp.101.2.345>
- Brown, T. (2001). Optical fibers and Fiber-optic communications. In M. Bass, JM. S. Enoch, EWW. tryland, & W. Wolfe (Eds.), *Handbook of Optics* (Second, Vol. 4, pp. 1.3-1.51). The McGraw-Hill, Companies Inc.

- Camarillo, D. B., Milne, C. F., Carlson, C. R., Zinn, M. R., & Salisbury, J. K. (2008). Mechanics modeling of tendon-driven continuum manipulators. *IEEE Transactions on Robotics*, 24(6). <https://doi.org/10.1109/TRO.2008.2002311>
- Carton, F.-X., Chabanas, M., le Lann, F., & Noble, J. H. (2020). Automatic segmentation of brain tumor resections in intraoperative ultrasound images using U-Net. *Journal of Medical Imaging*, 7(03). <https://doi.org/10.1117/1.jmi.7.3.031503>
- Ceccarini, F., Guerra, S., Peressotti, A., Peressotti, F., Bulgheroni, M., Baccinelli, W., Bonato, B., & Castiello, U. (2021). On-line control of movement in plants. *Biochemical and Biophysical Research Communications*, 564, 86–91. <https://doi.org/10.1016/j.bbrc.2020.06.160>
- Chen, S., Sun, L., Zhou, X., Guo, Y., Song, J., Qian, S., Liu, Z., Guan, Q., Meade Jeffries, E., Liu, W., Wang, Y., He, C., & You, Z. (2020). Mechanically and biologically skin-like elastomers for bio-integrated electronics. *Nature Communications*, 11(1). <https://doi.org/10.1038/s41467-020-14446-2>
- Chikhaoui, M. T., & Burgner-Kahrs, J. (2018). Control of continuum robots for medical applications: State of the art (invited review). *ACTUATOR 2018 - 16th International Conference and Exhibition on New Actuators and Drive Systems, Conference Proceedings*.
- Chirikjian GS. (1992). *Theory and applications of hyper-redundant robotic manipulators* [California Institute of Technology]. <https://doi.org/DOI: 10.7907/F12D-0X25>
- Choi, H. R., Jung, K., Ryew, S., Nam, J. do, Jeon, J., Koo, J. C., & Tanie, K. (2005). Biomimetic soft actuator: Design, modeling, control, and applications. *IEEE/ASME Transactions on Mechatronics*, 10(5). <https://doi.org/10.1109/TMECH.2005.856108>
- Dagenais, P., Hensman, S., Haechler, V., & Milinkovitch, M. C. (2021). Elephants evolved strategies reducing the biomechanical complexity of their trunk. *Current Biology*, 31(21). <https://doi.org/10.1016/j.cub.2021.08.029>
- Dong, X., Raffles, M., Cobos-Guzman, S., Axinte, D., & Kell, J. (2016). A novel continuum robot using twin-Pivot compliant joints: Design, modeling, and validation. *Journal of Mechanisms and Robotics*, 8(2). <https://doi.org/10.1115/1.4031340>
- Du, X., Lin, X., Wang, C., Zhou, K., Wei, Y., & Tian, Z. (2022). Endoscopic surgery versus craniotomy in the treatment of spontaneous intracerebral hematoma: a systematic review and meta-analysis. *Chi Neurosurg J*., 8(1), 1–12.
- Ebel, F., Greuter, L., Guzman, R., & Soleman, J. (2022). Resection of brain lesions with a neuroendoscopic ultrasonic aspirator – a systematic literature review. *Neurosurg Rev*., 45(5), 3109–3118.
- Emile, O., le Floch, A., & Vollrath, F. (2007). Time-resolved torsional relaxation of spider draglines by an optical technique. *Physical Review Letters*, 98(16). <https://doi.org/10.1103/PhysRevLett.98.167402>
- Feng, F., Hong, W., & Xie, L. (2020). Design of 3D-Printed Flexible Joints with Presetable Stiffness for Surgical Robots. *IEEE Access*, 8. <https://doi.org/10.1109/ACCESS.2020.2991092>
- Feng, Y., Ide, T., Nabae, H., Endo, G., Sakurai, R., Ohno, S., & Suzumori, K. (2021). Safety-enhanced control strategy of a power soft robot driven by hydraulic artificial muscles. *ROBOMECH Journal*, 8(1). <https://doi.org/10.1186/s40648-021-00194-5>
- Foroughi, J., Spinks, G. M., Aziz, S., Mirabedini, A., Jeiranikhameneh, A., Wallace, G. G., Kozlov, M. E., & Baughman, R. H. (2016). Knitted Carbon-Nanotube-Sheath/Spandex-Core Elastomeric Yarns for Artificial Muscles and Strain Sensing. *ACS Nano*, 10(10). <https://doi.org/10.1021/acsnano.6b04125>
- Gandhi, H. (2022). Experimental Endoscope Rotitome-C: A pixel-by-pixel erasure microsurgical endoscopic sarcotome for resection of soft tissue tumours in closed body cavities. *International Journal of Computer and Technology*, 22(Open Access), 147–170.
- Gandhi, H. S. (2022). Hyalite Sol-Gel Amoeba: A Physiology-Based Biophysical Model for Segmentation and Biotransformation of Medical Images To 3D Solid-State Characterizing Native Tissue Properties for Patient-Specific and Patient-Appropriate Analysis for Surgical Applications. *INTERNATIONAL JOURNAL OF COMPUTERS & TECHNOLOGY*, 22, 64–85. <https://doi.org/10.24297/ijct.v22i.9228>
- George Thuruthel, T., Ansari, Y., Falotico, E., & Laschi, C. (2018). Control Strategies for Soft Robotic Manipulators: A Survey. In *Soft Robotics* (Vol. 5, Issue 2). <https://doi.org/10.1089/soro.2017.0007>
- Gerard, I. J., Kersten-Oertel, M., Petrecca, K., Sirhan, D., Hall, J. A., & Collins, D. L. (2017). Brain shift in neuronavigation of brain tumors: A review. In *Medical Image Analysis*. <https://doi.org/10.1016/j.media.2016.08.007>

- Gifari, M. W., Naghibi, H., Stramigioli, S., & Abayazid, M. (2019). A review on recent advances in soft surgical robots for endoscopic applications. In *International Journal of Medical Robotics and Computer Assisted Surgery* (Vol. 15, Issue 5). <https://doi.org/10.1002/rcs.2010>
- Grant, B. D., Quang, T., Possati-Resende, J. C., Scapulatempo-Neto, C., de Macedo Matsushita, G., Mauad, E. C., Stoler, M. H., Castle, P. E., Guerreiro Fregnani, J. H. T., Schmeler, K. M., & Richards-Kortum, R. (2019). A mobile-phone based high-resolution microendoscope to image cervical precancer. *PLoS ONE*. <https://doi.org/10.1371/journal.pone.0211045>
- Gu, G. Y., Zhu, J., Zhu, L. M., & Zhu, X. (2017). A survey on dielectric elastomer actuators for soft robots. In *Bioinspiration and Biomimetics* (Vol. 12, Issue 1). <https://doi.org/10.1088/1748-3190/12/1/011003>
- Hall, J. (2016a). *Guyton and Hall textbook of Medical Physiology* (13 International). Elsevier Inc.
- Hall, J. (2016b). *Guyton and Hall textbook of Medical Physiology* (13 International). Elsevier Inc.
- Hannan, M. W., & Walker, I. D. (2003). Kinematics and the implementation of an elephant's trunk manipulator and other continuum style robots. *Journal of Robotic Systems*, 20(2). <https://doi.org/10.1002/rob.10070>
- Hao, G., Dai, F., He, X., & Liu, Y. (2017). Design and analytical analysis of a large-range tri-symmetrical 2R1T compliant mechanism. In *Microsystem Technologies* (Vol. 23, Issue 10). <https://doi.org/10.1007/s00542-017-3423-8>
- Hartkens, T., Hill, D. L. G., Castellano-Smith, A. D., Hawkes, D. J., Maurer, C. R., Martin, A. J., Hall, W. A., Liu, H., & Truwit, C. L. (2003). Measurement and analysis of brain deformation during neurosurgery. *IEEE Transactions on Medical Imaging*. <https://doi.org/10.1109/TMI.2002.806596>
- Hassan, T., Cianchetti, M., Mazzolai, B., Laschi, C., & Dario, P. (2017). Active-Braid, a Bioinspired Continuum Manipulator. *IEEE Robotics and Automation Letters*, 2(4). <https://doi.org/10.1109/LRA.2017.2720842>
- Heckman, C., & Enoka, R. (2012). Motor Unit. *Comprehensive Physiology*, 2(4), 2629–2682.
- Hopkins H, & Kapany NS. (1954). A Flexible Fibrescope, using Static Scanning. *Nature*, 173, 39–41.
- Howie C, Lynch K, Hutchinson, S., Kantor G, Wolfram B, Kavradi L, & Thrun S. (2005). *Principles of Robot Motion: Theory, Algorithms, and Implementations*. The MIT Press.
- Isbister, A., Bailey, N. Y., & Georgilas, I. (2021). An Integrated Kinematic Modeling and Experimental Approach for an Active Endoscope. *Frontiers in Robotics and AI*, 8. <https://doi.org/10.3389/frobt.2021.667205>
- Jacobs I. (2001). Optical fiber communication Technologies and system overview. In M. Bass, JM. Enoch, EWW. Stryland, & W. Wolfe (Eds.), *Handbook of Optics* (second, Vol. 4, pp. 2.1-2.16). The McGraw-Hill, Companies Inc.
- J.Hecht. (2004). City of light – the story of fibre optics. In *Optics and Lasers in Engineering*.
- Karan, S. K., Maiti, S., Kwon, O., Paria, S., Maitra, A., Si, S. K., Kim, Y., Kim, J. K., & Khatua, B. B. (2018). Nature driven spider silk as high energy conversion efficient bio-piezoelectric nanogenerator. *Nano Energy*, 49. <https://doi.org/10.1016/j.nanoen.2018.05.014>
- Kato, T., Okumura, I., Kose, H., Takagi, K., & Hata, N. (2016). Tendon-driven continuum robot for neuroendoscopy: validation of extended kinematic mapping for hysteresis operation. *International Journal of Computer Assisted Radiology and Surgery*, 11(4). <https://doi.org/10.1007/s11548-015-1310-2>
- Khuri-Yakub, B. T., & Oralkan, Ö. (2011). Capacitive micromachined ultrasonic transducers for medical imaging and therapy. *Journal of Micromechanics and Microengineering*. <https://doi.org/10.1088/0960-1317/21/5/054004>
- Kier, W. M. (2012). The diversity of hydrostatic skeletons. In *Journal of Experimental Biology* (Vol. 215, Issue 8). <https://doi.org/10.1242/jeb.056549>
- Kier, W. M., & Smith, K. K. (1983). The biomechanics of movement in tongues and tentacles. *Journal of Biomechanics*, 16(4). [https://doi.org/10.1016/0021-9290\(83\)90176-8](https://doi.org/10.1016/0021-9290(83)90176-8)
- KIER, W. M., & SMITH, K. K. (1985). Tongues, tentacles and trunks: the biomechanics of movement in muscular-hydrostats. *Zoological Journal of the Linnean Society*, 83(4). <https://doi.org/10.1111/j.1096-3642.1985.tb01178.x>
- Kier, W. M., & Stella, M. P. (2007). The arrangement and function of octopus arm musculature and connective tissue. *Journal of Morphology*, 268(10). <https://doi.org/10.1002/jmor.10548>

- Kim, Y., Cheng, S. S., Diakite, M., Gullapalli, R. P., Simard, J. M., & Desai, J. P. (2017). Toward the development of a flexible mesoscale MRI-compatible neurosurgical continuum robot. *IEEE Transactions on Robotics*, 33(6). <https://doi.org/10.1109/TRO.2017.2719035>
- Kinoshita, M., Kijima, N., Kagawa, N., & Kishima, H. (2021). The exoscope paradigm shift in neurosurgery. *Japanese Journal of Neurosurgery*, 30(3). <https://doi.org/10.7887/jcns.30.199>
- Klute, G. K., Czerniecki, J. M., & Hannaford, B. (1999). McKibben artificial muscles: Pneumatic actuators with biomechanical intelligence. *IEEE/ASME International Conference on Advanced Intelligent Mechatronics, AIM*. <https://doi.org/10.1109/aim.1999.803170>
- Kumar, B., & Singh, K. P. (2014). Fatigueless response of spider draglines in cyclic torsion facilitated by reversible molecular deformation. *Applied Physics Letters*, 105(21). <https://doi.org/10.1063/1.4902942>
- Langer, M., Amanov, E., & Burgner-Kahrs, J. (2018). Stiffening sheaths for continuum robots. *Soft Robotics*, 5(3). <https://doi.org/10.1089/soro.2017.0060>
- Li, K. W., Nelson, C., Suk, I., & Jallo, G. I. (2005). Neuroendoscopy: past, present, and future. In *Neurosurgical focus* (Vol. 19, Issue 6). <https://doi.org/10.3171/foc.2005.19.6.2>
- Li, M., Kang, R., Geng, S., & Guglielmino, E. (2018). Design and control of a tendon-driven continuum robot. *Transactions of the Institute of Measurement and Control*, 40(11). <https://doi.org/10.1177/0142331216685607>
- Li, S., & Hao, G. (2021). Current trends and prospects in compliant continuum robots: A survey. In *Actuators* (Vol. 10, Issue 7). <https://doi.org/10.3390/act10070145>
- Li, T., Li, Y., & Zhang, T. (2019). Materials, Structures, and Functions for Flexible and Stretchable Biomimetic Sensors. *Accounts of Chemical Research*, 52(2). <https://doi.org/10.1021/acs.accounts.8b00497>
- Luo, M., Skorina, E. H., Tao, W., Chen, F., Ozel, S., Sun, Y., & Onal, C. D. (2017). Toward modular soft robotics: Proprioceptive curvature sensing and sliding-mode control of soft bidirectional bending modules. *Soft Robotics*, 4(2). <https://doi.org/10.1089/soro.2016.0041>
- Manti, M., Cacucciolo, V., & Cianchetti, M. (2016). Stiffening in soft robotics: A review of the state of the art. *IEEE Robotics and Automation Magazine*, 23(3). <https://doi.org/10.1109/MRA.2016.2582718>
- Marchese, A. D., Katzschmann, R. K., & Rus, D. (2014). Whole arm planning for a soft and highly compliant 2D robotic manipulator. *IEEE International Conference on Intelligent Robots and Systems*. <https://doi.org/10.1109/IROS.2014.6942614>
- Marcus, H. J., Seneci, C. A., Hughes-Hallett, A., Cundy, T. P., Nandi, D., Yang, G. Z., & Darzi, A. (2016). Comparative Performance in Single-Port Versus Multiport Minimally Invasive Surgery, and Small Versus Large Operative Working Spaces. *Surgical Innovation*, 23(2). <https://doi.org/10.1177/1553350615610650>
- Meijer, K., Rosenthal, M. S., & Full, R. J. (2001). Muscle-like actuators? A comparison between three electroactive polymers. *Smart Structures and Materials 2001: Electroactive Polymer Actuators and Devices*, 4329. <https://doi.org/10.1117/12.432649>
- Moosa, S., Ding, D., Mastorakos, P., Sheehan, J. P., Liu, K. C., & Starke, R. M. (2018). Endoport-assisted surgical evacuation of a deep-seated cerebral abscess. *Journal of Clinical Neuroscience*, 53. <https://doi.org/10.1016/j.jocn.2018.04.028>
- Motkoski, J., & Sutherland, G. (2014). Progress in Neurosurgical Robotics. In F. A. Jolesz (Ed.), *Intraoperative Imaging and Image-Guided Therapy* (ed, pp. 601–612). Springer Science+Business Media.
- Nakaji, P., & Spetzler, R. F. (2004). Innovations in surgical approach: the marriage of technique, technology, and judgment. *Clinical Neurosurgery*.
- Ota, T., Degani, A., Schwartzman, D., Zubiato, B., McGarvey, J., Choset, H., & Zenati, M. A. (2009). A Highly Articulated Robotic Surgical System for Minimally Invasive Surgery. *Annals of Thoracic Surgery*, 87(4). <https://doi.org/10.1016/j.athoracsur.2008.10.026>
- Ozel, S., Skorina, E. H., Luo, M., Tao, W., Chen, F., Pan, Y., & Onal, C. D. (2016). A composite soft bending actuation module with integrated curvature sensing. *Proceedings - IEEE International Conference on Robotics and Automation, 2016-June*. <https://doi.org/10.1109/ICRA.2016.7487703>
- Pelrine, R., Kornbluh, R., Qibing, P., Stanford, S., Seajin, O., Eckerle, J., Full, R. J., Rosenthal, M., & Meijer, K. (2017). Dielectric Elastomer Artificial Muscle Actuators: Toward Biomimetic Motion. *Smart Structures and Materials*, 4695.

- Pernecky, A., Reisch, R., & Kindel, S. (1994). *Concept and Surgical Technique: Keyhole Approaches in Neurosurgery* (Vol. 1). Springer 2008.
- Prochazka, A., & Ellaway, P. (2012). Sensory systems in the control of movement. In *Comprehensive Physiology* (Vol. 2, Issue 4). <https://doi.org/10.1002/cphy.c100086>
- Proske, U., & Gandevia, S. (2012). The proprioceptive senses: their roles in signaling body shape, body position and movement, and muscle force. *Physiol Rev*. 2012 Oct;92(4):1651-97, 92(4), 1651-1697.
- Reisch, R., Stadie, A., Kockro, R. A., & Hopf, N. (2013). The keyhole concept in neurosurgery. In *World Neurosurgery* (Vol. 79, Issue 2 SUPPL.). <https://doi.org/10.1016/j.wneu.2012.02.024>
- Renda, F., Boyer, F., Dias, J., & Seneviratne, L. (2018). Discrete Cosserat Approach for Multisection Soft Manipulator Dynamics. *IEEE Transactions on Robotics*, 34(6). <https://doi.org/10.1109/TRO.2018.2868815>
- Rigante, L., Borghesi-Razavi, H., Recinos, P. F., & Roser, F. (2019). An overview of endoscopy in neurologic surgery. In *Cleveland Clinic Journal of Medicine* (Vol. 86, Issue 10). <https://doi.org/10.3949/ccjm.86.me.18142>
- Rigneault, H., Andresen, E., Kudlinski, A., & Bouwmans, G. (2018). New fiber probes for biosensing and imaging. *Optics InfoBase Conference Papers, Part F111-SOF 2018*. <https://doi.org/10.1364/SOF.2018.SoW1H.1>
- Sayehmiri, F., Starke, R. M., Eichberg, D. G., Ghanikolahloo, M., Rahmatian, A., Fathi, M., Vakili, K., Ebrahimzadeh, K., Rezaei, O., Samadian, M., Mousavinejad, S. A., Maloumeh, E. N., Tavasol, H. H., & Sharifi, G. (2022). Comparison of microscopic and endoscopic resection of third-ventricular colloid cysts: A systematic review and meta-analysis. In *Clinical Neurology and Neurosurgery* (Vol. 215). <https://doi.org/10.1016/j.clineuro.2022.107179>
- Shaikh, S., & Deopujari, C. (2020). The endoscope and instruments for minimally invasive neurosurgery. *Mini-Invasive Surgery, 2020*. <https://doi.org/10.20517/2574-1225.2020.97>
- Shehata, N., Kandas, I., Hassounah, I., Sobolčiak, P., Krupa, I., Mrlik, M., Popelka, A., Steadman, J., & Lewis, R. (2018). Piezoresponse, mechanical, and electrical characteristics of synthetic spider silk nanofibers. *Nanomaterials*, 8(8). <https://doi.org/10.3390/nano8080585>
- Shim, K. W., Park, E. K., Kim, D. S., & Choi, J. U. (2017). Neuroendoscopy: Current and future perspectives. In *Journal of Korean Neurosurgical Society* (Vol. 60, Issue 3). <https://doi.org/10.3340/jkns.2017.0202.006>
- Singh, I., Rohilla, S., Kumar, P., & Krishana, G. (2018). Combined microsurgical and endoscopic technique for removal of extensive intracranial epidermoids. *Surgical Neurology International*, 9(1). https://doi.org/10.4103/sni.sni_392_17
- Sionkowska, A. (2011). Current research on the blends of natural and synthetic polymers as new biomaterials: Review. In *Progress in Polymer Science (Oxford)* (Vol. 36, Issue 9). <https://doi.org/10.1016/j.progpolymsci.2011.05.003>
- Song, Y., Li, M., Sun, L., & Qin, L. (2006). A novel miniature mobile robot system for micro operation task. *9th International Conference on Control, Automation, Robotics and Vision, 2006, ICARCV '06*. <https://doi.org/10.1109/ICARCV.2006.345347>
- Standring, S. (2008). Gray's Anatomy: The anatomical basis of clinical practice. In *Edinburg. Elsevier Churchill Livingstone*. <https://doi.org/10.1017/CBO9781107415324.004>
- Stevanovic, M. v, & Sharpe, F. (2017). Green's operative hand surgery. In *Green's Operative Hand Surgery*.
- Steven, E., Park, J. G., Paravastu, A., Lopes, E. B., Brooks, J. S., Englander, O., Siegrist, T., Kaner, P., & Alamo, R. G. (2011). Physical characterization of functionalized spider silk: Electronic and sensing properties. *Science and Technology of Advanced Materials*, 12(5). <https://doi.org/10.1088/1468-6996/12/5/055002>
- Steven, E., Saleh, W. R., Lebedev, V., Acquah, S. F. A., Laukhin, V., Alamo, R. G., & Brooks, J. S. (2013). Carbon nanotubes on a spider silk scaffold. *Nature Communications*, 4. <https://doi.org/10.1038/ncomms3435>
- Tammam, M., Khayat, R. E., Khallaf, M., & Hassan, M. H. (2022). The endoscopic-assisted approach versus the microscopic only approach in resection of cerebellopontine angle epidermoids: a 5-year retrospective study. *Egypt J Neurol Psychiatry Neurosurg*, 58, 1-5.
- Tan, T. K., Merola, J., Zaben, M., Gray, W., & Leach, P. (2021). Neuroendoscopy versus Craniotomy in Basal Ganglia Haemorrhage: A Systematic Review and Meta-Analysis. *British Journal of Surgery*, 108(Supplement_6). <https://doi.org/10.1093/bjs/zxab258>

- Tan, T. K., Merola, J., Zaben, M., Gray, W., & Leach, P. (2022). Craniotomy versus endoscopic approach in basal ganglia haemorrhage: A systematic review and meta-analysis. *Neurology Asia*, 27(1), 45–62. <https://doi.org/10.54029/2022nzf>
- Tondu, B., Boitier, V., & Lopez, P. (1994). Naturally compliant robot-arms actuated by McKibben artificial muscles. *Proceedings of the IEEE International Conference on Systems, Man and Cybernetics*, 3. <https://doi.org/10.1109/icsmc.1994.400269>
- Trivedi, D., Rahn, C. D., Kier, W. M., & Walker, I. D. (2008). Soft robotics: Biological inspiration, state of the art, and future research. *Applied Bionics and Biomechanics*, 5(3). <https://doi.org/10.1080/11762320802557865>
- Trout, J. M., Walsh, E. J., & Fayer, R. (2002). Rotifers Ingest Giardia Cysts. *The Journal of Parasitology*. <https://doi.org/10.2307/3285557>
- Tuchman, A., Platt, A., Winer, J., Pham, M., Giannotta, S., & Zada, G. (2014). Endoscopic-assisted resection of intracranial epidermoid tumors. In *World Neurosurgery* (Vol. 82, Issues 3–4). <https://doi.org/10.1016/j.wneu.2013.03.073>
- Vollrath, F., & Knight, D. P. (2001). Liquid crystalline spinning of spider silk. In *Nature* (Vol. 410, Issue 6828). <https://doi.org/10.1038/35069000>
- Vollrath, F., Madsen, B., & Shao, Z. (2001). The effect of spinning conditions on the mechanics of a spider's dragline silk. *Proceedings of the Royal Society B: Biological Sciences*, 268(1483). <https://doi.org/10.1098/rspb.2001.1590>
- Wallace, R. L. (2002). Rotifers: Exquisite metazoans. *Integrative and Comparative Biology*.
- Webster, R. J., Okamura, A. M., & Cowan, N. J. (2006). Toward active cannulas: Miniature snake-like surgical robots. *IEEE International Conference on Intelligent Robots and Systems*. <https://doi.org/10.1109/IROS.2006.282073>
- Webster, R. J., Romano, J. M., & Cowan, N. J. (2009). Mechanics of precurved-tube continuum robots. *IEEE Transactions on Robotics*, 25(1). <https://doi.org/10.1109/TRO.2008.2006868>
- Wickham, J. (1987). The new surgery. *Br Med J (Clin Res Ed)*. 1987 Dec;295(6613):1581–2, 295(6613), 1581–1582.
- Yan, C., Yan, H., & Jin, W. (2021). Application of Endoport-Assisted Neuroendoscopic Techniques in Lateral Ventricular Tumor Surgery. *Research Square*.
- Yang, C., Geng, S., Walker, I., Branson, D. T., Liu, J., Dai, J. S., & Kang, R. (2020). Geometric constraint-based modeling and analysis of a novel continuum robot with Shape Memory Alloy initiated variable stiffness. *International Journal of Robotics Research*, 39(14). <https://doi.org/10.1177/0278364920913929>
- Yang, Y., Wu, Y., Li, C., Yang, X., & Chen, W. (2020). Flexible Actuators for Soft Robotics. *Advanced Intelligent Systems*, 2(1). <https://doi.org/10.1002/aisy.201900077>
- Youn, J. H., Jeong, S. M., Hwang, G., Kim, H., Hyeon, K., Park, J., & Kyung, K. U. (2020). Dielectric elastomer actuator for soft robotics applications and challenges. *Applied Sciences (Switzerland)*, 10(2). <https://doi.org/10.3390/app10020640>
- Yun, S., Park, S., Park, B., Ryu, S., Jeong, S. M., & Kyung, K. U. (2020). A soft and transparent visuo-haptic interface pursuing wearable devices. *IEEE Transactions on Industrial Electronics*, 67(1). <https://doi.org/10.1109/TIE.2019.2898620>
- Zhao, B., Zhang, W., Zhang, Z., Zhu, X., & Xu, K. (2018). Continuum Manipulator with Redundant Backbones and Constrained Bending Curvature for Continuously Variable Stiffness. *IEEE International Conference on Intelligent Robots and Systems*. <https://doi.org/10.1109/IROS.2018.8593437>
- Zhao, H., Huang, R., & Shepherd, R. F. (2016). Curvature control of soft orthotics via low cost solid-state optics. *Proceedings - IEEE International Conference on Robotics and Automation, 2016-June*. <https://doi.org/10.1109/ICRA.2016.7487590>
- Zhao, Y., & Chen, X. (2016). Endoscopic treatment of hypertensive intracerebral hemorrhage: A technical review. *Chronic Diseases and Translational Medicine*, 2(3). <https://doi.org/10.1016/j.cdtm.2016.11.002>

Appendix

Table: Materials and their mechanical properties.

Source: The elaborate structure of spider silk (2008), doi: [10.4161/pri.2.4.7490](https://doi.org/10.4161/pri.2.4.7490).

	Material density (g cm ³)	Strength (GPa)	Elasticity (%)	Toughness (MJ m ³)
Steel	7.8	1.5	0.8	6.0
Carbon fibre	1.8	4.0	1.3	25
Kevlar 49	1.4	3.6	2.7	5.0
MA silk	1.3	1.1	27	180
Flag silk	1.3	0.5	270	150
Insect silk	1.3	0.6	18	70
Nylon 6.6	1.1	0.95	18	80